

# Convex Polytopes: Extremal Constructions and $f$ -Vector Shapes

Günter M. Ziegler

## Introduction

These lecture notes treat some current aspects of two closely interrelated topics from the theory of convex polytopes: the shapes of  $f$ -vectors, and extremal constructions.

The study of  $f$ -vectors has had huge successes in the last forty years. The most fundamental one is undoubtedly the “ $g$ -theorem,” conjectured by McMullen in 1971 and proved by Billera & Lee and Stanley in 1980, which characterizes the  $f$ -vectors of simplicial and of simple polytopes combinatorially. See also Section ?? of Forman’s article in this volume, where  $h$ -vectors are discussed in connection with the Charney–Davis conjecture. Nevertheless, on some fundamental problems embarrassingly little progress was made; one notable such problem concerns the shapes of  $f$ -vectors of 4-polytopes.

A number of striking and fascinating polytope *constructions* has been proposed and analyzed over the years. In particular, the Billera–Lee construction produces “all possible  $f$ -vectors” of simplicial polytopes. Less visible progress was made outside the range of simple or simplicial polytopes — where our measure of progress is that new polytopes “with interesting  $f$ -vectors” should be produced. Thus, still “it seems that overall, we are short of examples. The methods for coming up with

---

<sup>1</sup>Institute of Mathematics, MA 6-2, TU Berlin, D-10623 Berlin, Germany.

**E-mail address:** ziegler@math.tu-berlin.de.

Partially supported by the Deutsche Forschungs-Gemeinschaft (DFG), via the Research Center MATHEON “Mathematics in the Key Technologies”, the Research Groups “Algorithms, Structure, Randomness” and “Polyhedral Surfaces”, and a Leibniz grant.

useful examples in mathematics (or counterexamples to commonly believed conjectures) are even less clear than the methods for proving mathematical statements” (Gil Kalai, 2000).

These lecture notes are meant to display a fruitful interplay of these two areas of study: The discussion of  $f$ -vector shapes suggests the notion of “extremal” polytopes, that is, of polytopes with “extremal  $f$ -vector shapes.” Our choice of constructions to be discussed here is guided by this: We will be looking at constructions that produce interesting  $f$ -vector shapes.

After treating 3-polytopes in the first lecture and the  $f$ -vector shapes of very high-dimensional polytopes in the second one, we will start to analyze the case of 4-dimensional polytopes in detail. Thus the third lecture will explain a surprisingly simple construction for 2-simple 2-simplicial 4-polytopes, which have symmetric  $f$ -vectors. Lecture four sketches the geometry of the cone of  $f$ -vectors for 4-polytopes, and thus identifies the existence/construction of 4-polytopes of high “fatness” as a key problem. In this direction, the last lecture presents a very recent construction of “projected products of polygons,” whose fatness reaches  $9 - \varepsilon$ . This shows that, on the topic of  $f$ -vectors of 4-polytopes, there is a narrowing gap between “the constraints we know” and “the examples we can construct.”

### Sources and Acknowledgements

The main sources, and the basis for the presentation in these lecture notes, are as follows. The proof of Steinitz’ theorem in Lecture 1 is due to Alexander Bobenko and Boris Springborn [17]. A detailed report about the work by Ludwig Danzer, Anders Björner, Carl Lee, Jürgen Eckhoff and many others (Lecture 2) appears in [79, Sect. 8.6]; see also [13] and [15]. The “deep vertex truncation” construction presented in Lecture 3 is from joint work with Andreas Paffenholz [57]; my understanding of 2-simple 2-simplicial polytopes benefits also from my previous work with David Eppstein and Greg Kuperberg [26]. Lecture 4 draws heavily on my 2002 Beijing ICM report [80], which was relying on previous studies by Marge Bayer [11], and with Andrea Höppner [42]. Finally, the construction presented in Lecture 5 was announced in [81]; the intuition for it was built in previous joint work with Nina Amenta [4] and Michael Joswig [43].

Nikolaus Witte and Thilo Schröder have forcefully directed the problem sessions for my Utah lectures, and suggested a number of exercises. Nikolaus Witte has prepared many, and the nicest, figures for these notes. The construction of many of the examples and the beautiful Schlegel diagram graphics are based on the `polymake` system by Evgenij Gawilow and Michael Joswig [31] [32] [33], which everyone is invited and recommended to try out, and use. An introduction to `polymake`, by Nikolaus Witte and Thilo Schröder, appears as an appendix, pp. 63–67.

I am grateful to all these colleagues for their work, for their explanations and critical comments, and for support on these lectures as well as in general. I have benefitted a lot from the lively discussions at the PCMI after my lectures, and from the many interesting questions and diverse feedback I got. Boris Springborn, Nikolaus Witte, Günter Rote, and many others provided very helpful comments on the draft version of these lecture notes. Thank you all!

More than usually, for the trip to Utah I have depended on the support, care, and love of Torsten Heldmann. Without him, I wouldn’t have been able to go.

## LECTURE 1

### Constructing 3-Dimensional Polytopes

All the *polytopes* considered in these lecture notes are convex. A  $d$ -*polytope* is a  $d$ -dimensional polytope; thus the 3-dimensional polytopes to be discussed in this lecture are plainly *3-polytopes*.\*

How many 3-dimensional polytopes “do we know”? When pressed for examples, we will perhaps start with the platonic solids: the regular tetrahedron, cube and octahedron, icosahedron and dodecahedron.

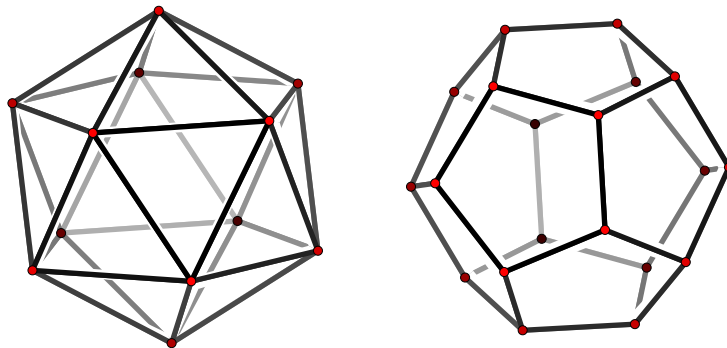


**Figure 1.1.** The regular icosahedron and dodecahedron

The classes of *stacked* and *cyclic* polytopes are of great importance for high-dimensional polytope theory because of their extremal  $f$ -vectors (according to the *lower bound theorem* and the *upper bound theorem*): Stacked polytopes arise from a simplex by repeatedly stacking pyramids onto the facets (cf. Lecture 2); cyclic polytopes are constructed as the convex hull of  $n > d$  points on a curve of order  $d$ . However, neither of these constructions produces particularly impressive objects in dimension 3 (compare Figure 1.2, and Exercise 1.8).

The same must be said about pyramids and bipyramids over  $n$ -gons ( $n \geq 3$ ) — see Figure 1.3.

---

\*We assume that the readers are familiar with the basic terminology and discrete geometric concepts; see e.g. [79, Lect. 0] or [40].

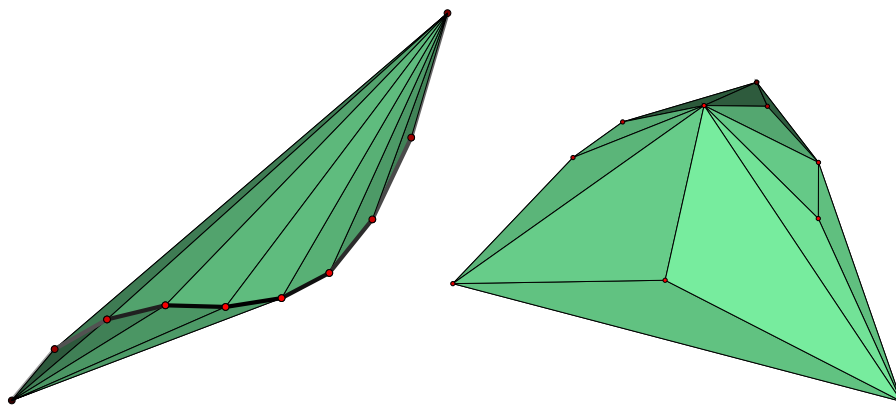


**Figure 1.2.** A cyclic 3-polytope  $C_3(10)$  and a stacked 3-polytope, with 10 vertices each

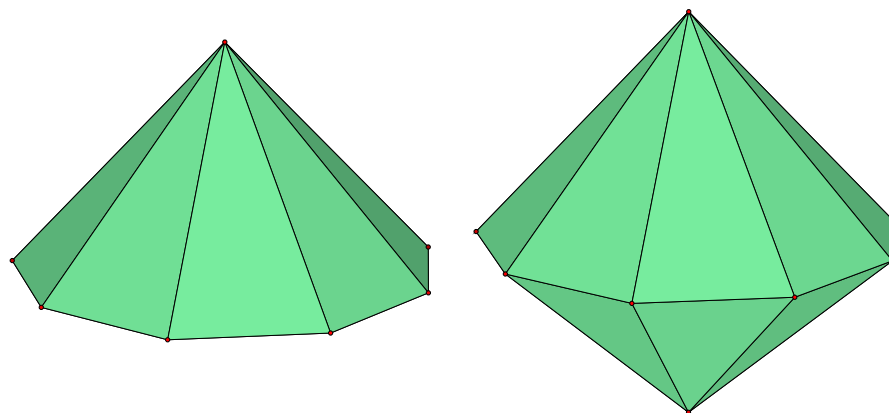


**Figure 1.3.** The pyramid and the bipyramid over a regular 10-gon

How do we get a “random” 3-polytope with lots of vertices? An obvious thing to look at is the convex hull of  $n$  random points on a 2-sphere.

Why is this not satisfactory? First, it produces only simplicial polytopes (with probability 1), and secondly it does not even produce all possible combinatorial types of simplicial 3-polytopes — see [39, Sect. 13.5]. It is a quite non-trivial problem to randomly produce all combinatorial types of polytopes of specified size (say, with a given number of edges). With the Steinitz theorem discussed below this reduces to a search for a random planar 3-connected graph with a given number of edges, say. See Schaeffer [64] for a recent treatment of this problem.

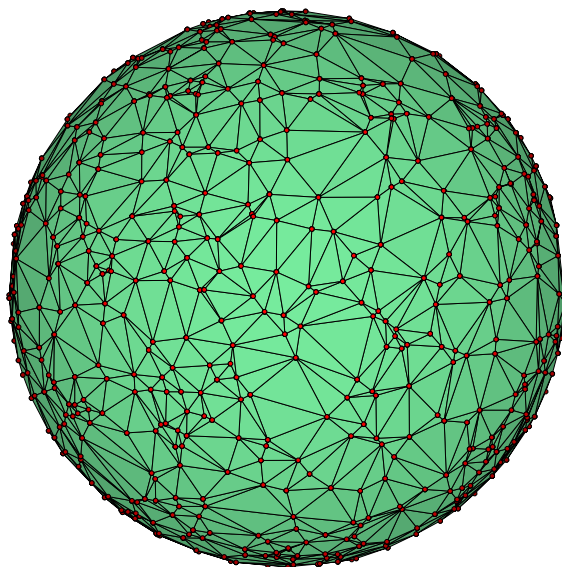


Figure 1.4. A random 3-polytope, with 1000 vertices on a sphere

### 1.1. The cone of $f$ -vectors

The  $f$ -vector of a 3-polytope  $P$  is the triplet of integers

$$f(P) = (f_0, f_1, f_2) \in \mathbb{Z}^3,$$

where  $f_0$  is the number of vertices,  $f_1$  is the number of edges, and  $f_2$  denotes the number of facets (2-dimensional faces). In view of Euler's equation  $f_0 - f_1 + f_2 = 2$  (which we take for granted here; but see Federico [27], Eppstein [25], and [2, Chap. 11]), the set of all  $f$ -vectors of 3-polytopes,

$\mathcal{F}_3 := \{(f_0, f_1, f_2) \in \mathbb{Z}^3 : f(P) = (f_0, f_1, f_2) \text{ is the } f\text{-vector of a 3-polytope } P\}$  is a 2-dimensional set. Thus  $\mathcal{F}_3$  is faithfully represented by the  $(f_0, f_2)$ -pairs of 3-polytopes,

$$\bar{\mathcal{F}}_3 := \{(f_0, f_2) \in \mathbb{Z}^2 : f(P) = (f_0, f_1, f_2) \text{ for some 3-polytope } P\},$$

as shown in Figure 1.5: The missing  $f_1$ -component is given by  $f_1 = f_0 + f_2 - 2$ .

The set of all  $f$ -vectors of 3-polytopes was completely characterized by a young Privatdozent at the Technische Hochschule Berlin-Charlottenburg (now TU Berlin), Ernst Steinitz, in 1906: In a simple two-and-a-half-page paper he obtained the following result, whose proof we leave to you (Exercise 1.3).

**Lemma 1.1** (Steinitz' lemma [73]). *The set of all  $f$ -vectors of 3-polytopes is given by*

$$\mathcal{F}_3 := \{(f_0, f_1, f_2) \in \mathbb{Z}^3 : f_0 - f_1 + f_2 = 2, f_2 \leq 2f_0 - 4, f_0 \leq 2f_2 - 4\}.$$

This answer to the  $f$ -vector problem for 3-polytopes is remarkably simple:  $\mathcal{F}_3$  is the set of *all* integral points in a 2-dimensional convex polyhedral cone. The three constraints that define the cone have clear interpretations: They are the Euler equation  $f_0 - f_1 + f_2 = 2$ , the upper bound inequality  $f_2 \leq 2f_0 - 4$ ,

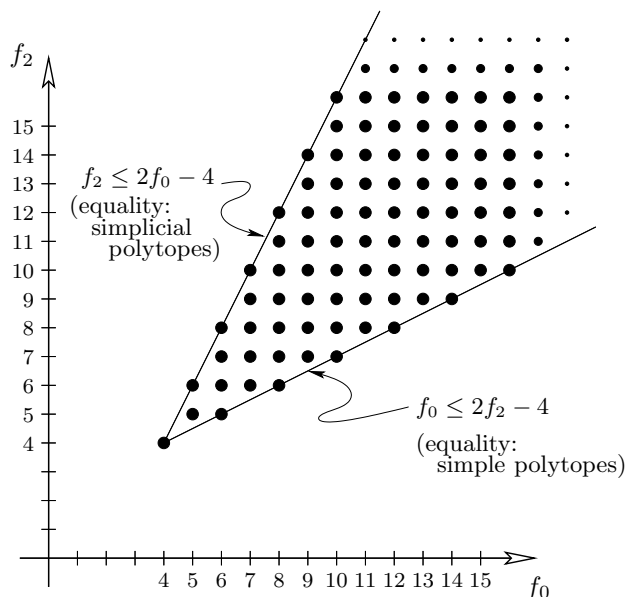


**Figure 1.5.** The set  $\bar{\mathcal{F}}_3$ , according to Steinitz' Lemma 1.1

which is tight exactly for the  $f$ -vectors of simplicial polytopes, and its dual,  $f_0 \leq 2f_2 - 4$ , which in the case of equality characterizes the  $f$ -vectors of simple 3-polytopes.

For the centennial of Steinitz' lemma, in 2006, let's strive for a characterization of the *cone* spanned by the  $f$ -vectors of 4-dimensional polytopes,  $\text{cone}(\mathcal{F}_4)$ . As we will see at the beginning of Lecture 4, this is a much more modest goal than a characterization of  $\mathcal{F}_4$ , which is not the set of all integral points in a convex set: It has "concavities" and even "holes."

Steinitz' lemma, as graphed in Figure 1.5, also shows that all ( $f$ -vectors of) convex 3-polytopes lie between the extremes of simple and of simplicial polytopes. And indeed, there seems to be the misconception that an analogous statement should be true in higher dimensions as well — it isn't. As we will see, there are additional interesting extreme cases in dimension 4, which are by far not as well understood as the simple and simplicial cases.

For any 3-polytope that is not a simplex, we may compute the "slope"

$$\phi(P) := \frac{f_2 - 4}{f_0 - 4}$$

it generates in the graph of Figure 1.5, with respect to the apex  $(4, 4)$  of the cone, which corresponds to a simplex. This slope satisfies

$$\frac{1}{2} \leq \phi(P) \leq 2,$$

where the lower bound characterizes simple polytopes, while the upper bound is tight for simplicial polytopes. Another interpretation of the parameter  $\phi$  is that it is a homogeneous coordinate for the cone, where the denominator  $f_0 - 4$  measures the "size" of the  $f$ -vector. ( $\phi$  is homogeneous, so it yields  $\frac{0}{0}$  for the  $f$ -vector of a simplex, which is the apex of the cone. Compare Exercise 1.5.)

## 1.2. The Steinitz theorem

While Steinitz' lemma from 1906 is a very simple result, his theorem from 1922, characterizing the graphs of 3-polytopes, is substantial and deep. He knew that: He called it the "Fundamentalsatz der konvexen Typen," the fundamental theorem of convex types. Here is an informal version of it.

**Theorem 1.2** (Steinitz' theorem [74, 75]). *There is a bijection*

$$\{\text{3-connected planar graphs}\} \longleftrightarrow \{\text{combinatorial types of 3-polytopes}\}.$$

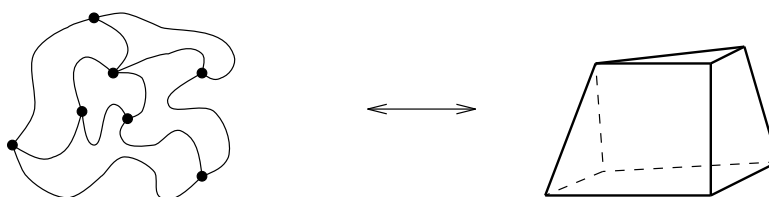


**Figure 1.6.** Graphs  $\longleftrightarrow$  polytopes, according to Steinitz' Theorem 1.2

The direction " $\longleftarrow$ " of Steinitz' theorem is not hard to establish.

Indeed, we do get a graph for any 3-polytope, namely the abstract graph whose nodes are the vertices of the polytope, and whose arcs are given by the edges of the polytope. This graph is indeed planar: To see this, one may first produce a radial projection of the polytope boundary (and thus of the vertices and edges) onto a sphere that contains the polytope, and then apply a stereographic projection [41, §36] to the plane. Or one may directly generate the "Schlegel diagram" and thus a straight-edge drawing of the graph in the plane. (In Lecture 3 we will see more of this tool, which shows its true power in the visualization of 4-polytopes.)

To see that the graph of any 3-polytope is 3-connected is also easy, using Menger's characterization of a  $d$ -connected graph as a graph that cannot be disconnected by removing or blocking less than  $d$  of its vertices. A powerful extension of this result is Balinski's theorem [6] [79, Thm. 3.14], that the graph of any  $d$ -polytope is  $d$ -connected.

Thus the hard and interesting part of Steinitz' theorem is the direction " $\longrightarrow$ ." It poses a non-trivial *construction problem*: To produce a convex 3-polytope with a prescribed graph (a geometric object) from an abstract planar graph (that is, from purely combinatorial data).

The first (easy) step for this is to convince oneself that the graph characterizes the complete combinatorial structure of the polytope. This follows from the simple observation (due to Whitney) that the faces of the polytope correspond exactly to the *non-separating induced cycles* in the graph.

Thus we have to construct convex 3-polytopes with prescribed combinatorics (face lattice), as given by a 3-connected planar graph. The importance of this step may be seen from the fact that three completely different types of proofs (and construction methods!) have been designed for it: Let's call them Steinitz type proofs, Tutte–Maxwell type proofs, and Koebe–Thurston type proofs.

*Steinitz type proofs.* Such proofs (of which Steinitz gave details on one in [74], and three are given in the Steinitz–Rademacher book [75] that appeared after Steinitz’ death), are based on the following principle. Any planar 3-connected graph can be “reduced” to the complete graph  $K_4$  by local operations, which yields a sequence

$$G = G_0 \rightarrow G_1 \rightarrow G_2 \rightarrow \dots \rightarrow G_{N-1} \rightarrow G_N = K_4.$$

of 3-connected planar graphs.

This reduction sequence should then be reversed: Starting with a simplex  $\Delta_3$  (with graph  $K_4$ ) we build up a sequence of polytopes,

$$P = P_0 \leftarrow P_1 \leftarrow P_2 \leftarrow \dots \leftarrow P_{N-1} \leftarrow P_N = \Delta_3,$$

where  $P_i$  is a 3-polytope with graph  $G_i$ , again by simple/local construction steps.

Such a proof is presented in detail in [79, Lect. 4], so there is no need to do this here. We just mention that a number of interesting extensions and corollaries may be derived from Steinitz type proofs. Indeed, Barnette & Grünbaum [9] proved that in the construction of the polytope  $P$ , the shape of one face of the polytope may be prescribed. For example, some hexagon face may be required to be a regular hexagon, which imposes a non-trivial additional constraint. Similarly, Barnette [7] proved with a Steinitz type argument that a “shadow boundary” may be prescribed:  $P$  may be constructed in such a way that from some view-point outside the polytope, the edges that bound the visible part of the surface of the polytope correspond to a prescribed simple cycle in the graph of the polytope (which need not be induced). Equivalently, we may construct  $P \subset \mathbb{R}^3$  so that the image  $\pi(P)$  of  $P$  under the orthogonal projection  $\pi : \mathbb{R}^3 \rightarrow \mathbb{R}^2$  is a polygon whose edges are given exactly by the edges of  $P$  that realize the prescribed cycle. Indeed, the edges must be “strictly preserved” by the projection, in the terminology that we will develop and use in Lecture 5.

*Tutte–Maxwell type proofs.* The Tutte–Maxwell approach to realizing 3-polytopes works in two stages: First one gets a “correct” drawing of the graph in the plane, then this drawing is lifted to 3-space.

For the first stage, one may assume that the graph contains a triangle face (if not, one dualizes; see Exercise 1.1). Then the vertices of this triangle are fixed in the plane, the edges are interpreted as ideal rubber bands, and the other vertices are placed according to the unique and easy-to-compute energy minimum, for which the sum of all squared edge lengths is minimal. This produces a correct, planar drawing of the graph without intersections — this is the (non-trivial) claim of Tutte’s (1963) “rubber band method” [77]; moreover, any such drawing can be lifted to three-space according to Maxwell–Cremona theory, which may be traced back to work by Maxwell [49] nearly one hundred years earlier (1864). We refer to Richter-Gebert [60, Sect. 13.1] for a modern treatment, with all the proofs.

The Tutte–Maxwell proofs also buy us non-trivial corollaries: Indeed, each combinatorial type of 3-polytope can be realized with rational coordinates, and thus even with integral vertex coordinates (by clearing denominators). One can derive from a Tutte–Maxwell proof that singly-exponential vertex coordinates suffice for this: After a number of improvements on the original estimates by Onn & Sturmfels [52] we now know that each type of an  $n$  vertex 3-polytope with a triangle face can be represented with vertex coordinates in  $\{0, 1, 2, \dots, \lfloor 28.45^n \rfloor\}$  (see [72], [61] and [59]). It is not clear whether polynomial-size vertex coordinates can be achieved.



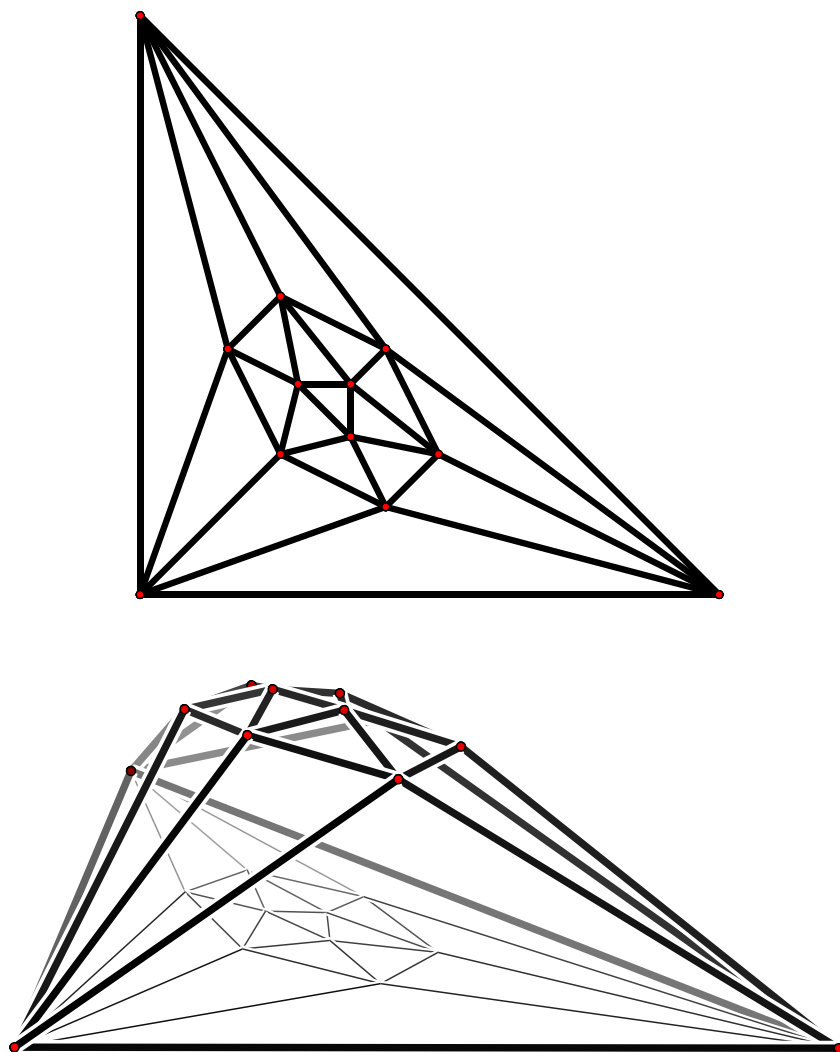


**Figure 1.7.** A Tutte drawing of the icosahedron graph, and the corresponding Maxwell–Cremona lifting

*Koebe–Thurston type proofs.* Geometric realizations of 3-polytopes *with all edges tangent to the sphere* may be derived from planar circle packings. Moreover, such a representation is essentially unique.

This seems to be essentially due to Bill Thurston [76] — who traces it back to Paul Koebe’s [46] work on complex functions, and to work by E. M. Andreev [5] from the sixties on hyperbolic polyhedra. Thurston’s insight was followed up, explained, extended and generalized by a number of authors. Pach & Agarwal [53, Chap. 8] describe the “standard” proof, based on a (non-constructive) fixed point

argument. However, Mohar [50] described an effective construction algorithm, and Colin de Verdière [20] was the first to prove that the circle packings in question can be derived from a variational principle (that is, an energy functional). In this line of work, Bobenko & Springborn [17] have quite recently discovered an explicit, elegant and quite general variational principle for the construction of circle patterns with prescribed intersection angles. In the following, we prove the Steinitz theorem based on their functional — taking advantage of all the simplifications that occur in their proof and formulas if one wants to “just” get the orthogonal circle patterns needed for the Steinitz theorem. (See also Springborn [68] for an additional discussion of uniqueness.)

### 1.3. Steinitz’ theorem via circle packings

**Theorem 1.3** (The Koebe–Andreev–Thurston theorem). *Each 3-connected planar graph can be realized by a 3-polytope which has all edges tangent to the unit sphere.*

*Moreover, this realization is unique up to Möbius transformations (projective transformations that fix the sphere). The edge-tangent realization for which the barycenter of the tangency points is the center of the sphere is unique up to orthogonal transformations.*

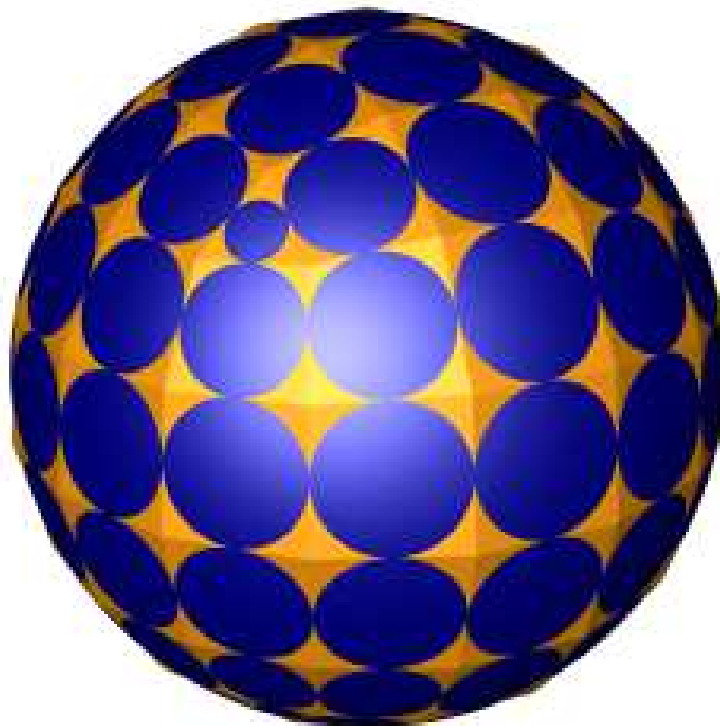
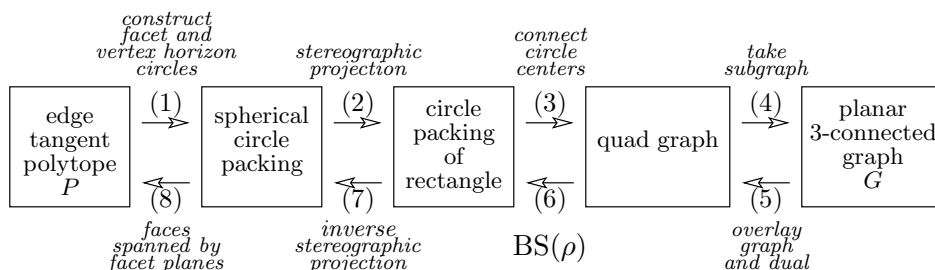


**Figure 1.8.** Edge-tangent representation of a polyhedron, according to the Koebe–Andreev–Thurston theorem [Graphics by Boris Springborn, MATHEON]

In our presentation of the proof, we first explain how any edge-tangent representation of a polytope  $P$  induces a circle pattern on the sphere, which in turn yields a planar circle pattern, and the combinatorics of the planar circle pattern yields a quad graph (a planar graph whose faces are quadrilaterals), which has  $G(P)$  as a subdivided subgraph. This yields steps (1) to (4) in the following scheme:



Our plan is to then reverse this four-step process, in order to construct an edge-tangent polytope from the given graph  $G$ . In step (5), the quad graph is derived directly from the graph  $G = G(P)$ , by superposing the graph with its dual. Then, in step (6), we construct the rectangular circle pattern with the combinatorics of the quad graph, and then proceed to construct  $P$  from it.

The steps (5), (7), and (8) are quite straightforward: The key, non-trivial step is (6), the construction of the (unique) rectangular circle pattern, which we achieve via the “euclidean Bobenko–Springborn functional.”

**Proof.** We start with a detailed description of the four-step process from edge-tangent polytopes to planar 3-connected graphs, via circle packings and quad graphs.

(1). Assume that  $P \subset \mathbb{R}^3$  is a 3-polytope whose edges are tangent to the unit sphere  $S^2 \subset \mathbb{R}^3$ . Then the facet planes of  $P$  intersect the unit sphere  $S^2$  in circles that we call the *facet circles*: We get one circle for each facet, and the circles are disjoint, but they touch exactly if the corresponding facets are adjacent. We also get a second set of circles which we call the *vertex horizon circles*: Each such circle is the boundary of the spherical cap consisting of all the points on the sphere that are “visible” from the respective vertex. We get one vertex horizon circle for each vertex, and the circles are disjoint, but they touch exactly if the corresponding vertices are adjacent.

Moreover, at each edge tangency point, the two touching facet circles and the two touching vertex horizon circles intersect orthogonally; see Figure 1.9 for an example. (The vertex horizon circles of  $P$  are the facet circles of the dual polytope  $P^*$ , whose edges have the same tangency points as the edges of  $P$ ; the facet circles for  $P$  are also the vertex horizon circles for  $P^*$ ; corresponding edges  $e \subset P$  and  $e^* \subset P^*$  intersect orthogonally at the respective tangency point.)

(2). We perform a stereographic projection to the plane, using one of the edge tangency points  $p_0$  as the projection center, and mapping all the facet and vertex horizon circles to the equator plane corresponding to the projection point. In the resulting planar figure, the two facet circles through  $p_0$  yield two parallel lines (and after a rotation we may assume that these are horizontal); the two vertex horizon circles through  $p_0$  also yield two parallel lines, orthogonal to the first two (and thus

vertical). So we get a planar pattern that consists of four lines bounding an axis-parallel rectangle, and circles that touch resp. intersect orthogonally in the plane. This is the *rectangular circle pattern*.

If the faces adjacent to the edge  $f$  through  $p_0$  are an  $h_1$ -gon and an  $h_2$ -gon, then we get  $h_1 - 2$  resp.  $h_2 - 2$  circles along the horizontal edges of the rectangle. Similarly, if the end vertices of  $f$  have degrees  $v_1$  and  $v_2$ , then we get  $v_1 - 2$  resp.  $v_2 - 2$  circles along the vertical edges of the rectangle. The example that one obtains from the cube (Figure 1.9) is displayed in Figure 1.10.

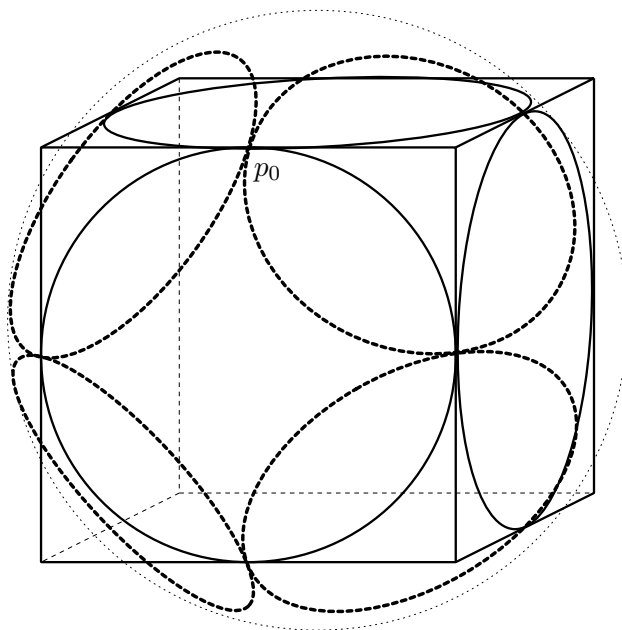


**Figure 1.9.** The facet circles and the vertex horizon circles (dashed) for an edge-tangent representation of a regular cube.

(3). Any rectangular circle pattern yields a quad graph drawing as follows: The vertex set consists of the centers of all the circles, with four additional vertices “far out” representing the four lines that bound the rectangles (as in Figure 1.11). We obtain drawings of both  $G$  and  $G^*$  by connecting the centers of touching facet circles resp. vertex horizon circles. This includes one horizontal edge  $f$  of  $G$  “going through infinity,” while dual graph  $G^*$  has the corresponding edge  $f^*$  going through infinity vertically.

From the rectangular circle pattern, we obtain a decomposition of a rectangle into quadrilaterals by connecting the centers of adjacent facet circles, and the centers of adjacent vertex horizon circles. See the example of Figure 1.11, where the rectangle is shaded. The graph of this rectangle decomposition is the *quad graph*: Its vertices correspond to (the centers of) the facet circles that don’t contain  $p_0$ , the vertex horizon circles that don’t contain  $p_0$ , and intersection points of edges  $e$  and  $e^*$  of  $G$  and  $G^*$ , other than the edges  $f, f^*$  that contain  $p_0$ .

(4). In particular, the graph  $G$  may be derived from the quad graph, by “deleting the dashed edges.”

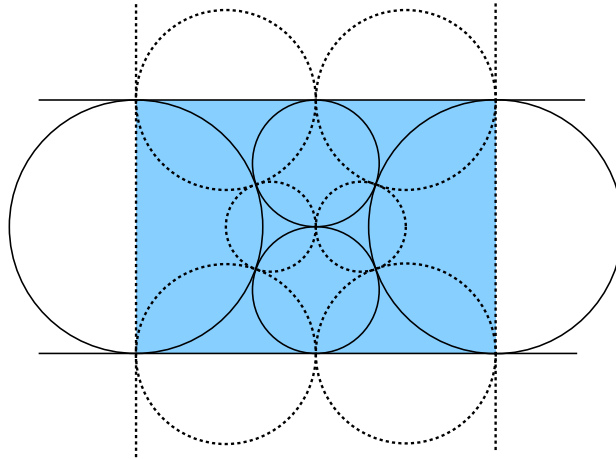


**Figure 1.10.** The rectangular circle pattern derived from an edge-tangent 3-cube (with  $h_1 = h_2 = 4$ ,  $v_1 = v_2 = 3$ )

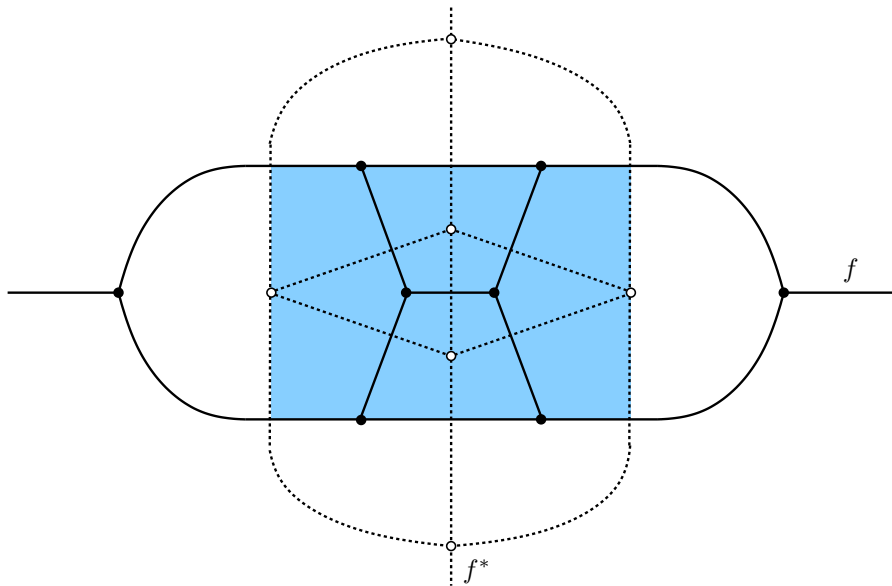


**Figure 1.11.** The quad graph for the cube, generated from Figure 1.10: The white vertices are given by the facet circle centers, while the black vertices correspond to the vertex horizon circles; the dashed edges connect the centers of adjacent facet circles, and the straight edges correspond to adjacent vertex horizon circles.

This ends the description of the passage from an edge tangent polytope to the planar graph drawing. Now we start the way back: Another four-step process leads us from graphs via quad graphs and circle patterns to edge-tangent 3-polytopes.

(5). The quad graph may be derived from knowledge of the graph  $G$  alone, plainly by overlaying  $G$  and  $G^*$ . For our cube example, the result may look like the drawing given in Figure 1.12.

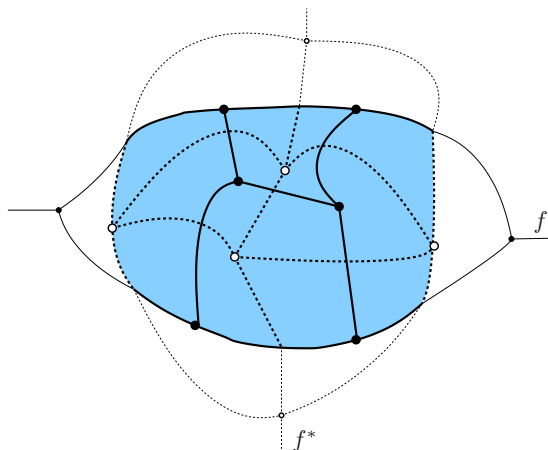


**Figure 1.12.** The quad graph for the cube, generated from an overlay of the cube graph (black edges) layed out with the edge  $f$  “at infinity” and the dual graph (dashed edges), with the dual edge  $f^*$  “at infinity.” The shaded part defines the restricted quad graph.

The input for the next step will be the *restricted quad graph*: It is obtained from the full quad graph by deleting everything that is adjacent to the original edges  $f$  and  $f^*$ . Its bounded faces are quadrilaterals (*quads* for short), with two black and two dashed edges each. Each quad has

- a *black* vertex and a *white* vertex  
(the black vertex, where the two black edges meet, corresponds to the center of a face circle; the white one, where the two dashed edges meet, corresponds to the center of a horizon circle),
- and two more vertices where a black and a dashed edge meet  
(they correspond to edge tangency points).

For the following, we use  $I_0$  as an indexing set for the black and white vertices in the restricted quad graph. It is in bijection with the vertices of  $G$  and of  $G^*$ , except for the vertices of the edges  $f$  and  $f^*$ , which yield lines rather than circles. That is, we have

$$I_0 := V(G - f) \cup V(G^* - f^*).$$

The following step, which takes us from combinatorics (a graph drawing) to geometry (a circle pattern), is the crucial one.

(6). In the “correct” realization of the restricted quad graph, which would yield a circle packing, each quad is drawn as a *kite* in which

- the two black edges have the same length  
(radius  $r_i$  of the corresponding vertex horizon circle),
- the two dashed edges have the same length  
(radius  $r_j$  of the corresponding facet circle),
- and there are two right angles between black and dashed edges  
(where facet and vertex horizon circles intersect).

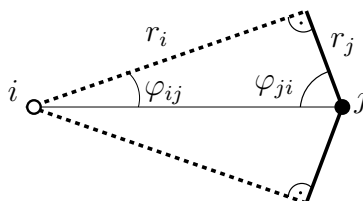


**Figure 1.13.** A kite, with radii  $r_i = e^{\rho_i}$ ,  $r_j = e^{\rho_j}$ , and angles  $\varphi_{ij}$  and  $\varphi_{ji}$

The kites have to look like the one in Figure 1.13.

Hence, we have to solve the following construction problem:

Given a quad graph decomposition of a rectangle, derived from the overlay of a 3-connected planar graph  $G$  and its dual  $G^*$ , construct a geometric drawing, with straight edges, as a kite decomposition of a rectangle.

The kites are completely determined if we know their edge lengths: If the edge lengths in a kite are  $r_i, r_j > 0$ , then the angles are given by

$$\varphi_{ij} = \arctan\left(\frac{r_j}{r_i}\right) \quad \text{and} \quad \varphi_{ji} = \arctan\left(\frac{r_i}{r_j}\right),$$

with  $\varphi_{ij} + \varphi_{ji} = \frac{\pi}{2}$  (see Figure 1.13). Thus all we have to do is to determine radii  $r_i$  corresponding to the black and white vertices of the quad graph, such that the following system of equations is satisfied:

$$(1.1) \quad \sum_{j : i \blacktriangleleft j} 2 \arctan\left(\frac{r_j}{r_i}\right) = \Phi_i \quad \text{for all vertices } i \in I_0,$$

where the right-hand-sides are given by

$$\Phi_i := \begin{cases} \pi & \text{if } i \text{ is on the boundary,} \\ 2\pi & \text{if } i \text{ is in the interior.} \end{cases}$$

In the equation whose right hand side is  $\Phi_i$ , the sum on the left hand side is taken over all vertices  $j \in I_0$  that are opposite to  $i$  in one of the kites. (If  $i$  is a white vertex, then  $j$  will be black, and vice versa.)

Indeed, if (1.1) is satisfied, then we can easily construct the kites and piece them together to get a flat rectangle and the circle packing. Badly enough, (1.1) is a non-linear system of equations, which we have to solve in positive variables  $r_i > 0$ . We want to know that this has a solution, which is unique up to multiplying all the  $r_i$ s with the same factor, and which can be computed efficiently. Luckily, we can do this, since the system is solved by minimizing an explicit and easy-to-write-down “energy” functional which will turn out to be convex, with a unique minimum. For this, we first do a change of variables,

$$\rho_i := \log r_i.$$

Then we normalize by the condition  $\prod_i r_i = 1$ , that is,

$$\sum_i \rho_i = 0.$$

Furthermore, we define

$$f(x) := \arctan(e^x).$$

This auxiliary function is graphed in Figure 1.14. Note that  $f(-x) = \frac{\pi}{2} - f(x)$ .

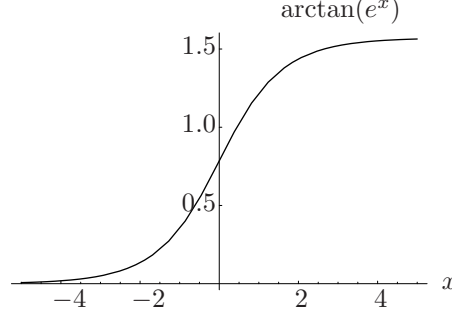


Figure 1.14.  $f(x) = \arctan e^x$

We differentiate  $f$ ,

$$f'(x) = \frac{1}{1 + e^{2x}} e^x = \frac{1}{2 \cosh x},$$

which yields  $f'(-x) = f'(x) > 0$  for all  $x \in \mathbb{R}$ . We also integrate  $f$ , and define

$$F(x) := \int_{-\infty}^x f(t) dt.$$

This function satisfies  $F(x) \geq 0$  for all  $x$ , but also  $F(x) \geq \frac{\pi}{2}x$ . Thus we get that

$$(1.2) \quad F(x) + F(-x) \geq \frac{\pi}{2}|x|.$$

The system (1.1) we have to solve may be rewritten in terms of  $f(x)$  as

$$(1.3) \quad \sum_{i : i \blacklozenge j} 2f(\rho_j - \rho_i) = \Phi_i \quad \text{for all black or white vertices, } i \in I_0.$$

To solve this, Bobenko & Springborn [17] present the functional

$$(1.4) \quad \text{BS}(\rho) := \sum_{i \blacklozenge j} \left\{ F(\rho_j - \rho_i) + F(\rho_i - \rho_j) - \frac{\pi}{2}(\rho_i + \rho_j) \right\} + \sum_{i \in I_0} \Phi_i \rho_i,$$

where the first sum is over all *unordered* pairs  $\{i, j\}$  of vertices  $i, j \in I_0$  that are opposite in one of the kites. The claim is now that

- (A) the critical points of  $\text{BS}(\rho)$  are exactly the solutions to our system (1.3),
- (B) the functional is convex: Restricted to  $\sum_i \rho_i = 0$  it is strictly positive definite, so the critical point is unique if it exists, and
- (C) the functional gets large if any of the differences  $\rho_i - \rho_j$  gets large: Thus the functional must have a critical point (a minimum) — the solution we are looking for.

For (A), a simple computation yields the gradient of  $\text{BS}(\rho)$ :

$$\frac{\partial \text{BS}(\rho)}{\partial \rho_i} = \Phi_i - \sum_{i \blacklozenge j} 2f(\rho_j - \rho_i).$$



Thus the critical points of  $\text{BS}(\rho)$  are exactly the solutions to (1.3).

For (B), we compute the Hessian (the matrix of second derivatives) for  $\text{BS}(\rho)$ , and find that

$$x^T \text{BS}(\rho)'' x = 2 \sum_{i \blacktriangleleft j} f'(\rho_j - \rho_i) (x_j - x_i)^2.$$

We know that  $f'(\rho_j - \rho_i) > 0$ , so this quadratic form can vanish only if all the differences  $x_j - x_i$  vanish for “adjacent”  $i, j \in I_0$  (that is, for black/white vertices that share a kite). But the graph we consider is connected, so this implies that all variables  $x_i$  are equal. Restricted to  $\sum_i x_i = 0$  this yields that all  $x_i$  vanish, so the Hessian is positive definite on the restriction hyperplane, and the solution we are striving for is unique if it exists.

To prove the existence claim (C), we have to find that  $\text{BS}(\rho)$  grows large if any difference of variables  $\rho_k - \rho_i$  gets large. With the same argument we just used this implies that some difference of “adjacent” variables will become large. Then also  $F(\rho_j - \rho_i) + F(\rho_i - \rho_j) \geq \frac{\pi}{2} |\rho_j - \rho_i|$  gets large, but it will grow only linearly in  $|\rho_j - \rho_i|$ , and it is not obvious that the growing positive terms in (1.4) will “outrun” the negative terms. This will require a careful “matching” between positive and negative terms.

To achieve this, we use the existence of a *coherent angle system*, that is, an assignment of angles  $\varphi_{ij}, \varphi_{ji} > 0$  to the kites that satisfies the conditions

$$(1.5) \quad \varphi_{ij} + \varphi_{ji} = \frac{\pi}{2} \quad \text{and} \quad \sum_{j : i \blacktriangleleft j} 2\varphi_{ij} = \Phi_i.$$

Any solution to (1.1) would give us a coherent angle system, but the existence of such a coherent angle system is much weaker, far from solving the system (1.1): If we have a coherent angle system, then we could construct kites from this — whose angles would fit together at the black and white vertices, but whose side lengths might not. (Compare Figure 1.15.)

For any coherent angle system,  $\varepsilon_0 := \min_{k, \ell} \varphi_{k\ell}$  is a positive number.

*If there is a coherent angle system, then the minimum exists.* Let’s assume for now that a coherent angle system exists (this will be proved below). Then

$$\begin{aligned} \text{BS}(\rho) &= \sum_{i \blacktriangleleft j} \left\{ F(\rho_j - \rho_i) + F(\rho_i - \rho_j) - \frac{\pi}{2}(\rho_i + \rho_j) \right\} + \sum_i \Phi_i \rho_i \\ &\stackrel{(i)}{>} \sum_{i \blacktriangleleft j} \left\{ \frac{\pi}{2} |\rho_i - \rho_j| - \frac{\pi}{2}(\rho_i + \rho_j) \right\} + \sum_i \Phi_i \rho_i \\ &\stackrel{(ii)}{=} \sum_{i \blacktriangleleft j} \left\{ \frac{\pi}{2} |\rho_i - \rho_j| - \frac{\pi}{2}(\rho_i + \rho_j) \right\} + \sum_{i \blacktriangleleft j} 2(\varphi_{ij} \rho_i + \varphi_{ji} \rho_j) \\ &\stackrel{(iii)}{=} \sum_{i \blacktriangleleft j} -\pi \min\{\rho_i, \rho_j\} + \sum_{i \blacktriangleleft j} 2(\varphi_{ij} \rho_i + \varphi_{ji} \rho_j) \\ &\stackrel{(iv)}{\geq} \sum_{i \blacktriangleleft j} -\pi \min\{\rho_i, \rho_j\} + \sum_{i \blacktriangleleft j} \pi \min\{\rho_i, \rho_j\} + 2 \min\{\varphi_{ji}, \varphi_{ij}\} |\rho_i - \rho_j| \\ &= \sum_{i \blacktriangleleft j} 2 \min\{\varphi_{ji}, \varphi_{ij}\} |\rho_i - \rho_j| \geq 2\varepsilon_0 \sum_{i \blacktriangleleft j} |\rho_i - \rho_j|. \end{aligned}$$

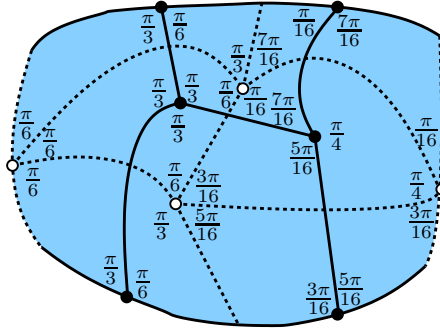


**Figure 1.15.** The assignment in this figure is a coherent angle system – but not one that corresponds to a correct circle pattern.

(Note that the construction of the coherent angle system proceeds from the plane graph without use of a straight edge drawing. In the figures further down we draw the graphs with straight edges for simplicity, but this structure is not used in the proof. Rather, it is produced by the proof.)

Here

- the estimate for (i) uses  $F(x) + F(-x) \geq \frac{\pi}{2}|x|$ , which is (1.2).
- (ii) is obtained by substituting (1.5). We need the second term in the second sum in (ii) since the sums over “ $i \diamond j$ ” are sums over unordered pairs; there is no extra summand for “ $j \diamond i$ .”
- (iii) follows from  $|x - y| - (x + y) = -2 \min\{x, y\}$ ,
- For (iv), in the case  $\rho_j \geq \rho_i$  we compute

$$\begin{aligned} 2(\varphi_{ij}\rho_i + \varphi_{ji}\rho_j) &= \pi\rho_i - 2\varphi_{ji}\rho_i + 2\varphi_{ji}\rho_j \\ &= \pi \min\{\rho_i, \rho_j\} + 2\varphi_{ji}|\rho_i - \rho_j| \\ &\geq \pi \min\{\rho_i, \rho_j\} + 2 \min\{\varphi_{ji}, \varphi_{ij}\}|\rho_i - \rho_j|, \end{aligned}$$

and analogously for  $\rho_i \geq \rho_j$ .

We are dealing with a connected quad graph. Thus if the norm of the vector  $\rho$  gets large, while the sum of the  $\rho_i$  is zero, then also for two  $i, j \in I_0$  in the same quadrilateral the difference  $|\rho_i - \rho_j|$  gets large. Thus by the computation above,  $\text{BS}(\rho) > 2\varepsilon_0|\rho_i - \rho_j|$  gets large. This is sufficient to prove that the strictly convex function  $\text{BS}(\rho)$  does have a (unique) minimum — the solution to our problem.

*A coherent angle system exists.* Finally, we have to verify the existence of a coherent angle system. We will see here that via some simple network flow theory, this follows from an expansion property in the “diagonal graph”  $D(G \cup G^*)$ . After that, we will prove the expansion property.

Let  $G$  be a 3-connected planar graph,  $G^*$  its dual, both of them again drawn into the plane with dual edges  $f, f^*$  intersecting “at infinity.” Then the *diagonal graph*  $D = D(G \cup G^*)$  has the same vertex set as  $G \cup G^*$ . Its edges correspond to the diagonals in the quad graph given by  $G \cup G^*$ .

Equivalently, the diagonal graph  $D$  has black vertices corresponding to the vertices of  $G$ , and white vertices corresponding to the faces of  $G$ . The edges of  $D$  correspond to the vertex–face incidences of  $G$ . See Figure 1.16 for an example.

The *reduced diagonal graph*  $D' = (V', E')$  is obtained from the diagonal graph  $D = (V, E)$  by removing the two vertices of  $f$ , the two vertices of  $f^*$ , and the four

edges that connect them, but none of the others. So indeed,  $D'$  does have pending edges (half-edges) which have lost one of their end-vertices.\* See Figure 1.17 for an example.

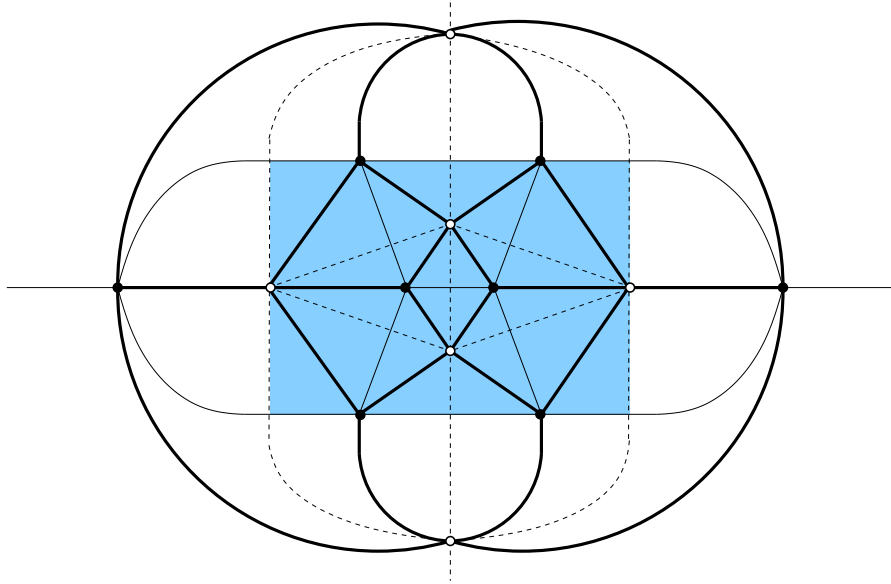


**Figure 1.16.** The diagonal graph  $D = D(G \cup G^*)$ , given by the fat edges, where  $G$  is the graph of the cube

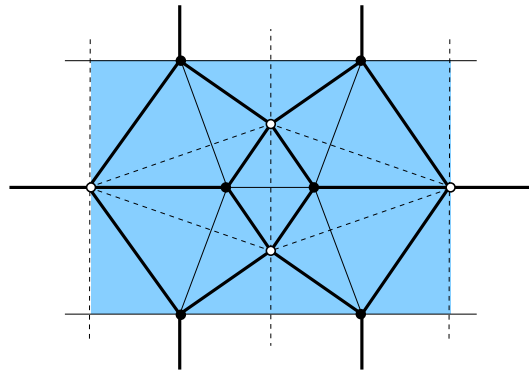


**Figure 1.17.** The fat edges in this figure display the reduced diagonal graph  $D' = D'(G \cup G^*)$  in the case where  $G$  is the graph of the cube, derived from Figure 1.16. Note that the fat edges leaving the rectangle are included in  $D'$ , their vertices at the other end are not. So in this example  $D'$  has 10 vertices and 20 edges, including 6 half-edges with only one end-vertex.

\*I am sure you won't be troubled too much by the fact that this is not a graph in the usual technical sense, since it does have half-edges with only one end-point.

The diagonal graph  $D = D(V, E)$  is a quad graph: All its faces, including the “unbounded” face (if we draw it in the plane) are quadrilaterals. From this, we get by double counting that  $|F| = 2|E|$  and thus  $|V| = 2|E| - 4$  by Euler’s relation. The reduced quad graph  $D' = (V', E')$  has  $|V'| = |V| - 4$  vertices and  $|E'| = |E| - 4$  edges. Hence we get  $|E'| = 2|V'|$ : The reduced quad graph has exactly double as many edges as vertices.

The concept of a coherent angle system has a very nice interpretation in terms of the restricted diagonal graph: Each vertex  $v_i$  gets a weight of  $2\pi$ , and this has to be distributed to the edges  $e$  incident to  $v_i$  such that

- each edge  $e$  incident to  $v_i$  gets a positive part of the weight  $2\pi$  of  $v_i$ ,
- all of the weight  $2\pi$  of  $v_i$  is distributed to its incident edges, and
- the weights assigned to each edge sum to  $\pi$ .

Indeed, in such an assignment any half-edge clearly gets a weight of  $\pi$  from its only end-vertex, which corresponds to a boundary vertex of the restricted quad graph; thus the boundary vertex  $v_i$  distributes a weight of exactly  $\Phi_i = \pi$  to its other incident edges, that is, to the (diagonals of the) kites it is incident to. The vertices of  $D'$  without an incident half-edge correspond to interior vertices  $v_j$  of the restricted quad graph, so they have a weight/angle of  $\Phi_j = 2\pi$  to distribute to the incident edges/kites.

The “weight distribution problem” for the reduced diagonal graph  $D' = (V', E')$  may also be interpreted as a flow problem (cf. [1]): We have to find a maximal flow, of weight  $2\pi|V'| = \pi|E'|$ , in a two-layer network as depicted in Figure 1.18. It consists of a source node  $s$ , then a layer of nodes formed by the vertex set  $V'$  of  $D'$ , then a layer of nodes in bijection to the edge set  $E'$ , and then the sink node  $t$ . There are three groups of arcs: The arcs  $(s, v')$  emanating from the source all have an upper bound of  $2\pi$ ; the arcs of type  $(v', e')$ , where the edge  $e'$  is incident to  $v'$ , get an upper bound of  $\infty$ , while the arcs at the sink,  $(e', t)$ , have an upper bound of  $\pi$ .

We need a *positive* flow in this network; to get this, we put a small lower bound of  $\varepsilon > 0$  on each edge of type  $(v', e')$ , and 0 on all other edges. There is a *feasible flow* in this network with upper and lower bounds on each edge: For this, let the flow value be  $\varepsilon$  on each  $(v', e')$ -arc, and a suitable multiple of  $\varepsilon$  on the other arcs.

We need a positive flow of value  $2\pi|V'| = \pi|E'|$  in this network. There is a feasible flow, and no flow with a larger value than  $2\pi|V'|$  can exist due to the cuts that separate  $s$  or  $t$  from the rest of the network. Thus we can apply the following generalization of the Max-Flow Min-Cut Theorem on network flows. (You should prove this yourself: See Exercise 1.9.)

**Theorem 1.4** (Generalized Max-Flow Min-Cut Theorem; cf. [1, Sect. 6.7]).

*If an  $(s, t)$ -network with lower and upper bounds has a feasible flow, then the value of a maximal  $(s, t)$ -flow is the capacity of a minimal  $(s, t)$ -cut.*

The *capacity* of an  $(s, t)$ -cut in a network with upper and lower bounds is the sum on the upper bounds of the forward arcs, minus the sum of the lower bounds on the backward arcs across the cut. So in our example the cuts  $[\{s\}, V' \cup E' \cup \{t\}]$  and  $[\{s\} \cup V' \cup E', \{t\}]$  have capacity  $2\pi|V'| = \pi|E'|$ . Could there be a cut of smaller capacity? Any  $(s, t)$ -cut is of the form

$$[\{s\} \cup V'_1 \cup E'_1, V'_2 \cup E'_2 \cup \{t\}]$$

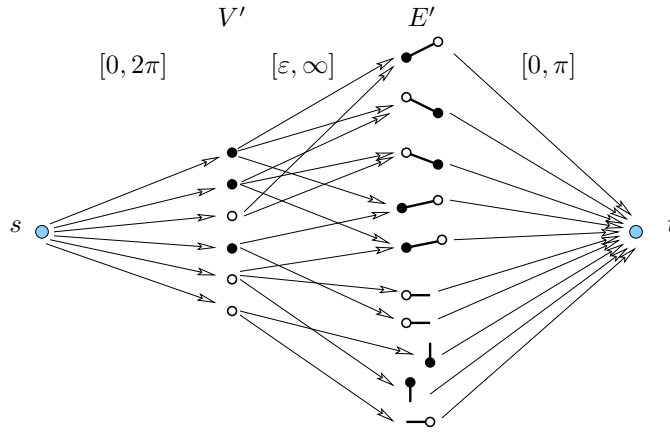


**Figure 1.18.** Construction of a coherent angle system from a network flow problem with lower and upper bounds, which are indicated by intervals like  $[0, \pi]$ .

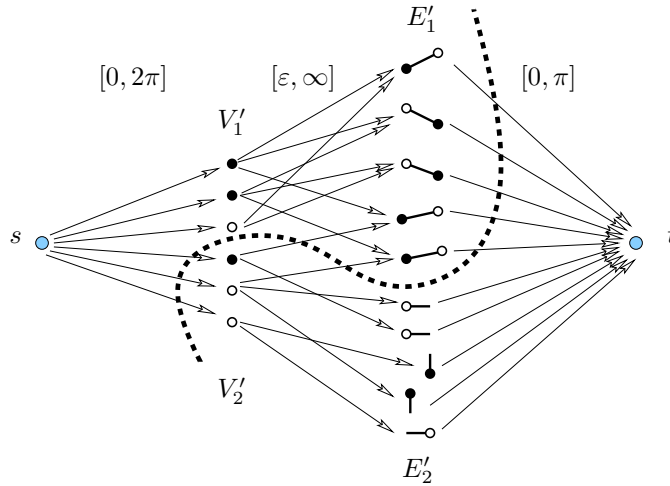


**Figure 1.19.** The dashed line indicates the cut  $[\{s\} \cup V'_1 \cup E'_1, V'_2 \cup E'_2 \cup \{t\}]$  in our network

for partitions  $V' = V'_1 \uplus V'_2$  and  $E' = E'_1 \uplus E'_2$ . Such a cut has finite capacity if there are no arcs  $(v', e')$  from  $V'_1$  to  $E'_2$ ; compare Figure 1.19. That is, we should take  $E'_1$  to include all the edges that are incident to a vertex in  $V'_1$ .

The capacity of the cut  $[\{s\} \cup V'_1 \cup E'_1, V'_2 \cup E'_2 \cup \{t\}]$  is

$$2\pi|V'_2| + \pi|E'_1| - \varepsilon|A(V'_2, E'_1)| = 2\pi|V'| - 2\pi|V'_1| + \pi|E'_1| - \varepsilon|A(V'_2, E'_1)|,$$

where  $|A(V'_2, E'_1)|$  denotes the number of arcs from  $V'_2$  to  $E'_1$ . For small enough  $\varepsilon$ , say  $\varepsilon = 1/|A(V', E')|$ , we have  $\varepsilon|A(V'_2, E'_1)| < 1$ . Thus the following “expansion property” for the diagonal graph implies that all cuts  $[\{s\} \cup V'_1 \cup E'_1, V'_2 \cup E'_2 \cup \{t\}]$  have capacity larger than  $2\pi|V'|$ , except in the two trivial cases given as examples above, where the capacity is exactly  $2\pi|V'|$ . Thus the maximal flow, of value  $2\pi|V'|$ , exists; it is positive, and yields the coherent angle system.

*Expansion in the diagonal graph.* It remains to verify the following: Let  $V'_1 \subseteq V'$  be a set of vertices in the reduced diagonal graph  $D'(G \cup G^*) = (V', E')$ , and assume that  $E'_1 \subseteq E'$  includes all edges of  $D'$  that are incident to a vertex in  $V'_1$ . Then

$$(1.6) \quad |E'_1| \geq 2|V'_1|,$$

with equality only in the trivial cases  $V'_1 = \emptyset$  and  $V'_1 = V'$ .

For this we may assume that the subgraph induced by  $V'_1$  is connected, because we can consider its components separately. We may also assume that  $|V'_1| \geq 2$ , so  $V'_1$  contains both a black and a white vertex.

Now let  $U$  be an open subset of the plane (or of  $S^2$ ) whose boundary curves separate  $V'_1$  from the  $h + 1$  components of the graph  $D \setminus V'_1$ , as illustrated in Figure 1.20. Topologically,  $U$  is an open disk with  $h \geq 0$  holes.

The diagonal graph yields a cell decomposition of  $U$ , consisting of  $f_0 = |V'_1|$  vertices,  $f_1^{\text{int}}$  interior edges,  $f_1^{\text{bdy}}$  other (half-)edges,  $q$  quadrilateral faces, and  $b_1 + b_2 + b_3$  boundary faces, where  $b_i$  counts the faces with  $i$  vertices in  $I'$ . In particular the total number of edges is  $f_1 = f_1^{\text{int}} + f_1^{\text{bdy}} = |E'_1|$ ,

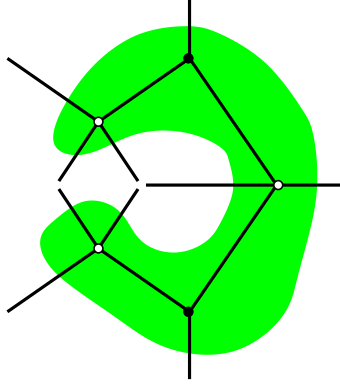


**Figure 1.20.** An example of five vertices in the reduced diagonal graph of Figure 1.17. The neighborhood  $U$  is shaded.

$f_0 = |V'_1| = 5$ ,  $f_1 = |E'_1| = 14$ ,  $f_1^{\text{int}} = 4$ ,  $f_1^{\text{bdy}} = 10$ ,  $h = 0$ ,  $q = 0$ ,  $b_1 = 4$ ,  $b_2 = 4$ ,  $b_3 = 2$ .

Double counting the edge-face incidences yields

$$(1.7) \quad 2f_1^{\text{int}} = 4q + b_2 + 2b_3 \quad \text{and} \quad 2f_1^{\text{bdy}} = 2b_1 + 2b_2 + 2b_3.$$

The Euler characteristic of  $U$  is

$$(1.8) \quad 1 - h = f_0 - f_1 + q + b_1 + b_2 + b_3 = f_0 - f_1^{\text{int}} + q.$$

With this we get

$$\begin{aligned} |E'_1| - 2|V'_1| &= f_1 - 2f_0 \stackrel{(1.8)}{=} (f_1^{\text{int}} + f_1^{\text{bdy}}) - 2(f_1^{\text{int}} - q + 1 - h) \\ &= f_1^{\text{bdy}} - f_1^{\text{int}} + 2q + 2h - 2 \\ &\stackrel{(1.7)}{=} (b_1 + b_2 + b_3) - (2q + \frac{1}{2}b_2 + b_3) + 2q + 2h - 2 \\ &= \frac{1}{2}(2b_1 + b_2 - 4) + 2h. \end{aligned}$$

To conclude that  $|E'_1| - 2|V'_1| \geq 0$ , with equality only if  $V'_1 = V'$ , we use  $h \geq 0$ , and need to verify that  $2b_1 + b_2 \geq 4$  holds, with equality only in the trivial case  $V'_1 = V'$ .

For this we count the vertices  $v$  of  $D \setminus V'_1$  which are *adjacent to*  $V'_1$ , that is, such that some quad in the full quad-graph  $D$  contains both  $v$  and a vertex from  $V'_1$ . Walking along the boundary curves of  $U$ , and exploring the quads that we traverse that way, we see that there are not more than  $2b_1 + b_2$  such vertices  $v$ : We find at most two new vertices in any quad that contains a boundary cell with 1 vertex in  $V'_1$ , and at most one new vertex in the quad of a boundary cell with 2 vertices in  $V'_1$ . The vertices found during the walk need not be all distinct, and some may not even lie outside  $V'_1$  (compare Figure 1.21). Thus we get only an inequality,

$$2b_1 + b_2 \geq \#\{\text{vertices of } D \setminus V'_1 \text{ adjacent to } V'_1\}.$$

In the boundary of each “hole” of  $U$  we will discover at least one vertex of  $D' \setminus V'_1$ . In the outer face during our walk we even discover a cycle of  $D$  (see Figure 1.21). Since  $D$  is bipartite, this cycle has even length. In the trivial case of  $V'_1 = V'$  this is exactly the 4-cycle  $C'$  given by  $D \setminus D'$ . If  $V'_1 \neq V'$ , then the vertices we discover either yield the cycle  $C'$  plus additional vertices, or we find a different cycle. But any cycle other than  $C'$  must have at least 6 vertices: Indeed, it is an even cycle, on which black and white vertices alternate. The black vertices on the cycle either include both the vertices of  $f$ , or with respect to the original graph  $G$  they separate a black vertex in  $V'_1$  from a vertex of  $f$ ; from the 3-connectivity of  $G$  we thus get that the cycle contains at least three black vertices, that is, at least 6 vertices in total. The same holds for the white vertices, the dual graph  $G^*$ , which is also 3-connected, and the vertices of  $f^*$ . Thus

$$\#\{\text{vertices of } D \text{ in the boundary of } U\} \geq 4,$$

with equality only if  $V'_1 = V'$ . This completes the proof for the expansion property, and thus for the existence of a coherent angle system, and of the circle packing.

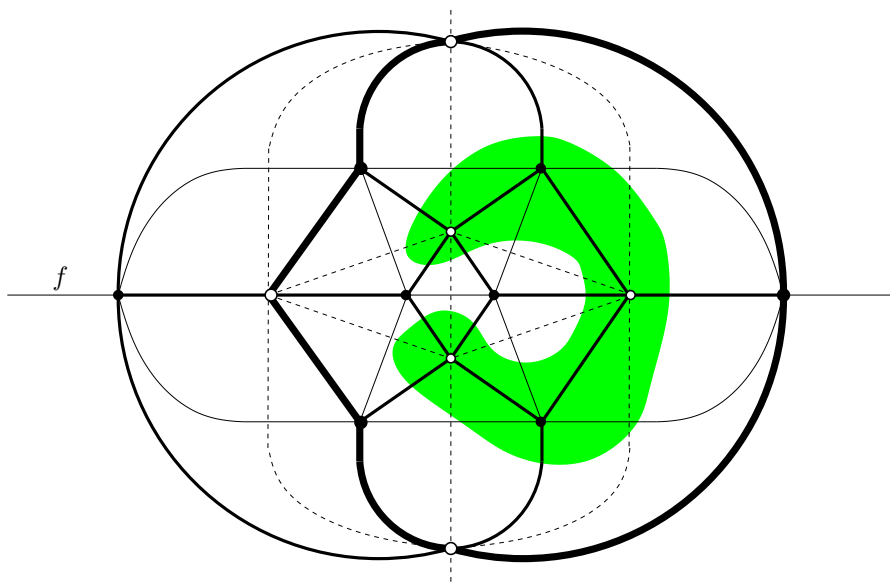


**Figure 1.21.** The cycle in the outer face to be discovered during the walk along the boundary curve of  $U$  is drawn with fat edges; it is a 6-cycle. With respect to  $G$ , which is drawn in thin black lines, the three vertices of the 6-cycle separate a vertex of  $f$  from the two black vertices in  $V'_1$ .

(7), (8). Given a correct rectangular circle pattern, it is easy to reconstruct the spherical circle pattern (via an inverse stereographic projection). From this, we obtain the edge-tangent polytope: Its face planes are given by the facet circles (and its vertices are given by the cone points for which the vertex horizon circles do indeed appear on the horizon). Thus construction steps (7) and (8) are easy — the hard part was (6).  $\square$

Is this the perfect proof? I think it is really nice, but still one could dream of a proof that avoids the stereographic projection, and produces the circle packing directly from some functional on the sphere . . . .

### Exercises

- 1.1. Show that each 3-polytope has a triangle face, or a simple vertex (a vertex of degree 3), or both. Even stronger, show that the number of triangle faces plus the number of simple vertices is at least eight, so there are at least four triangle faces, or at least four simple vertices.  
Hint: Use the Euler equation.
- 1.2. Prove that each 3-polytope has two faces with the same number of vertices.  
Hint: Do not use the Euler equation.
- 1.3. Prove the Steinitz Lemma 1.1:
  - Prove the “upper bound theorem” for dimension 3, that is, that  $f_2 \leq 2f_0 - 4$  (you may use Euler’s equation), and derive  $f_0 \leq 2f_2 - 4$  by duality.
  - Compute the  $f$ -vectors of the pyramids over  $n$ -gons.
  - How does  $(f_0, f_2)$  change if you stack a pyramid onto a triangle 2-face, or if you truncate a simple vertex?
- 1.4. If a 3-dimensional polytope has  $f_1 = 23$  edges, how many vertices/faces can it have? Construct an example for each possible pair  $(f_0, f_2)$ .
- 1.5. Alternative homogeneous coordinates for the cone of  $f$ -vectors are given by the “imbalance”  $\sigma := \frac{f_2 - f_0}{f_1 - 6}$ , where the self-dual term  $f_1 - 6$  measures the “size.” Show that  $-\frac{1}{3} \leq \sigma \leq +\frac{1}{3}$ , where  $\sigma = \pm\frac{1}{3}$  characterizes simple resp. simplicial polytopes.
- 1.6. Characterize the possible  $(f_0, f_2)$ -pairs for *cubical* 3-polytopes, that is, for all polytopes with quadrilateral 2-faces only. Where are the  $(f_0, f_2)$ -pairs of cubical 3-polytopes in Figure 1.5?  
How about 3-polytopes with pentagon faces only? Hexagon faces only?
- 1.7. Construct quad graphs and the planar circle patterns for
  - (a) a square pyramid,
  - (b) a cube/octahedron,
  - (c) a cube with vertex cut off,
  - (d) a dodecahedron.
 Which of the circle patterns do you get with rational coordinates?
- 1.8. Show that every 3-dimensional cyclic polytope  $C_3(n)$  is a stacked polytope. (However,  $C_d(n)$  is not stacked, for  $d \geq 4$  and  $n \geq d + 2$ .)
- 1.9. Describe a computational procedure to construct a coherent angle system: For this use a scheme to augment flows along undirected paths in the network with lower and upper bounds (increasing the value along forward arcs, decreasing the values on backward arcs). Your procedure should also imply a proof for the Generalized Max-Flow Min-Cut Theorem [1, Thm. 6.10, p. 193].



## LECTURE 2

### Shapes of $f$ -Vectors

Let's look at the  $f$ -vectors of  $d$ -dimensional convex polytopes  $P$ , where the dimension  $d$  is really large. Any such  $f$ -vector

$$\begin{aligned} f(P) &= (f_0, f_1, f_2, \quad \dots \quad \dots \quad \dots, f_{d-3}, f_{d-2}, f_{d-1}) \\ &= (\# \text{vertices}, \# \text{edges}, \# \text{2-faces}, \dots, \# \text{subridges}, \# \text{ridges}, \# \text{facets}) \end{aligned}$$

is a long sequence of large numbers, which we may graph just like a continuous function, and ask for its “shape.” Indeed, we might look at a shape function  $\varphi : [0, 1] \rightarrow \mathbb{R}$  that is defined by  $\varphi(x) := f_{x(d-1)}$ ; this is defined for any  $x = \frac{k}{d-1}$  that is a multiple of  $\frac{1}{d-1}$ , and these values are rather dense if  $d$  is large. We might interpolate if we want. But what types of  $f$ -vector shape functions  $\varphi$  do we get that way?

Figure 2.1 shows two “naive” views, of the shape of an  $f$ -vector, and — equivalently — of the shape of a typical face lattice (displayed as a *Hasse diagram*, so the sizes of rank levels are the  $f_i$ -values).

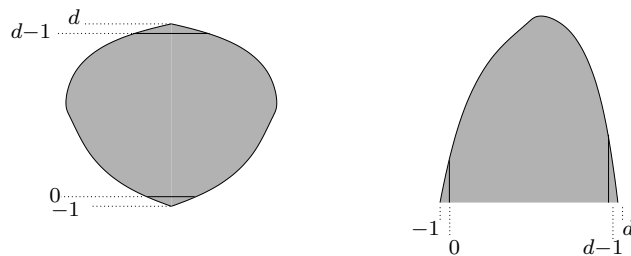


**Figure 2.1.** A rough, “naive” picture of the shape of the face lattice, and the  $f$ -vector, for a high-dimensional polytope

A very simple observation is that each vertex of a  $d$ -polytope has degree at least  $d$ , so double counting yields  $f_1 \geq \frac{d}{2}f_0 > f_0$ ; dually, we have  $f_{d-2} \geq \frac{d}{2}f_{d-1} > f_{d-1}$ . So in the first step, the  $f$ -sequence increases, in the last step it decreases. Does this mean that the  $f$ -vector “first goes up, then comes down,” that it is *unimodal*, with no “dip” in the middle?

## 2.1. Unimodality conjectures

Unimodality conjectures and theorems abound in combinatorics [71] [19]: for binomial coefficients, Stirling numbers and their generalizations, matroids and geometric lattices, etc. . . . The basic unimodality conjecture for convex polytopes was posed at least twice, by Theodore Motzkin in the late fifties, and by Dominic Welsh in 1972 (see [13]). Apparently it was disproved dramatically by Ludwig Danzer, already in the early sixties (presented in a lecture in Graz in 1964, according to Jürgen Eckhoff), but this is “lost mathematics,” no published account exists.

**Conjecture 2.1.** *The  $f$ -vectors of convex polytopes are unimodal, that is, for each  $d$ -polytope  $P$  there is an  $\ell = \ell(P)$  such that*

$$f_0 \leq f_1 \leq \cdots \leq f_\ell \geq \cdots \geq f_{d-2} \geq f_{d-1}.$$

The main point of this lecture will be to see that this is dead wrong, even for simplicial polytopes. Moreover, we want to see this “asymptotically,” without substantial amounts of computation, without having to list explicit  $f$ -vectors.

This asymptotic view is also motivated by the fact that the conjecture fails only in high dimensions. For example, for simplicial polytopes, it is true up to  $d = 19$ , and fails beyond this dimension. For general polytopes, we will see a counterexample for  $d = 8$ , but none are known for a smaller dimension. The conjecture holds in full for  $d \leq 4$  (Exercise 2.2), and also for  $d = 5$ , according to Werner [78].

Since the conjecture is so badly wrong, it might pay off to explicitly state what remains from it:

**Conjecture 2.2** (Björner [13] [15]). *The  $f$ -vectors of convex polytopes increase on the first quarter, and they decrease on the last quarter:*

$$f_0 < f_1 < \cdots < f_{\lceil \frac{d-1}{4} \rceil}, \quad f_{\lfloor \frac{3(d-1)}{4} \rfloor} > \cdots > f_{d-2} > f_{d-1}.$$

This is trivially true for  $d \leq 5$ . It also is true for *simplicial*  $d$ -polytopes (the  $f$ -vectors of simplicial polytopes indeed increase up to the middle, and they decrease in the last quarter), but the available proof for this depends on the necessity part of the  $g$ -theorem, so it is quite non-trivial; see [15].

To demonstrate our ignorance on such basic  $f$ -vector shape matters, here is a suspiciously innocuous conjecture. Apparently no one has an idea for a proof, up to now.

**Conjecture 2.3** (Bárány). *For any  $d$ -polytope,  $f_k \geq \min\{f_0, f_{d-1}\}$ .*

Bárány’s conjecture holds for  $d \leq 6$  [78]. However, not even

$$f_k \geq \frac{1}{10000} \min\{f_0, f_{d-1}\}$$

is proven for large dimensions  $d$ ! We know so little . . .

## 2.2. Basic examples

Let’s compute the  $f$ -vector shapes for the most basic high-dimensional polytopes that we can come up with. For rough estimates, we use a very crude version of Stirling’s formula,

$$n! \sim \left(\frac{n}{e}\right)^n.$$

**Example 2.4** (The simplex). For the  $(d-1)$ -simplex  $\Delta_{d-1}$  we have

$$f_{k-1}(\Delta_{d-1}) = \binom{d}{k}.$$

With logarithms taken with base 2,  $x := \frac{k}{d}$ , and  $\varphi(x) = f_{x d-1}$ , we get

$$\log \varphi(x) = \log \binom{d}{x d} \sim -x \log x - (1-x) \log(1-x).$$

A little bit of analysis shows from this that the  $f$ -vector is symmetric, with a sharp peak in the middle (at  $x = \frac{1}{2}$ ), of width  $\sim \frac{1}{\sqrt{d}}$ . Figure 2.2 displays a realistic example.

Of course, this is a well-known property of binomial coefficients, and the strong limit theorems of probability theory depend on it. (In this context  $\varphi(x)$  is known as the “entropy function.”)

**Example 2.5** (Cross polytopes). For the  $d$ -dimensional cross polytope  $C_d^* = \text{conv}\{\pm e_1, \dots, \pm e_d\}$  we have

$$f_k(C_d^*) = \binom{d}{k+1} 2^{k+1}.$$

Again, approximating crudely and taking logarithms base 2, we get

$$\log \varphi(x) \sim -x \log x - (1-x) \log(1-x) + x.$$

The derivative

$$\frac{d}{dx} \varphi(x) \sim -\log x - \frac{1}{\ln 2} + \log(1-x) + \frac{1}{\ln 2} + 1$$

vanishes at  $x = \frac{2}{3}$ : That’s where  $\log \varphi(x)$  has its maximum, and where  $\varphi(x)$  has a sharp peak (compare Figure 2.2).

Thus the  $f$ -vector of a  $d$ -dimensional cross polytope, for large  $d$ , has a sharp peak at  $k = \frac{2}{3}d$ . By duality, this means that the  $f$ -vector of the  $d$ -cube peaks at  $k = \frac{1}{3}d$ , for large  $d$ .

**Example 2.6** (Cyclic polytopes). Let’s look at cyclic polytopes  $C_d(n)$  with many vertices,  $n \gg d$ . For simplicity, we assume that the dimension  $d$  is even.

A curve in  $\mathbb{R}^d$  has degree  $d$  if no  $d+1$  points on the curve lie on a hyperplane. The convex hull of any  $n > d$  points on such a curve is a cyclic polytope  $C_d(n)$ . *Gale’s evenness criterion* [30] gives a combinatorial description for the facets, which is easy to visualize (see Figure 2.3): Any  $d$  points on a degree  $d$  curve span a hyperplane  $H$ . If the  $d$  points are supposed to span a facet of the polytope, then all the other  $n-d$  points must lie on the same side of  $H$ . Since the curve crosses  $H$  *only* in these  $d$  points, this means that the  $d$  points split into  $\frac{d}{2}$  adjacent pairs. So, if we number the points  $1, 2, \dots, n$  along the curve, then the facets of their convex hull (the cyclic polytope) are given by  $\frac{d}{2}$  pairs  $i, i+1 \pmod n$ . The  $(k-1)$ -faces are given by the  $k$ -subsets of such a  $d$ -set: For  $k \leq \frac{d}{2}$  any such subset will do (the cyclic polytopes are *neighborly*), while for  $k > \frac{d}{2}$  the faces consist of  $k - \frac{d}{2}$  pairs, and  $d-k$  singletons. Thus the  $(k-1)$ -faces may be obtained by choosing  $\frac{d}{2}$  vertices

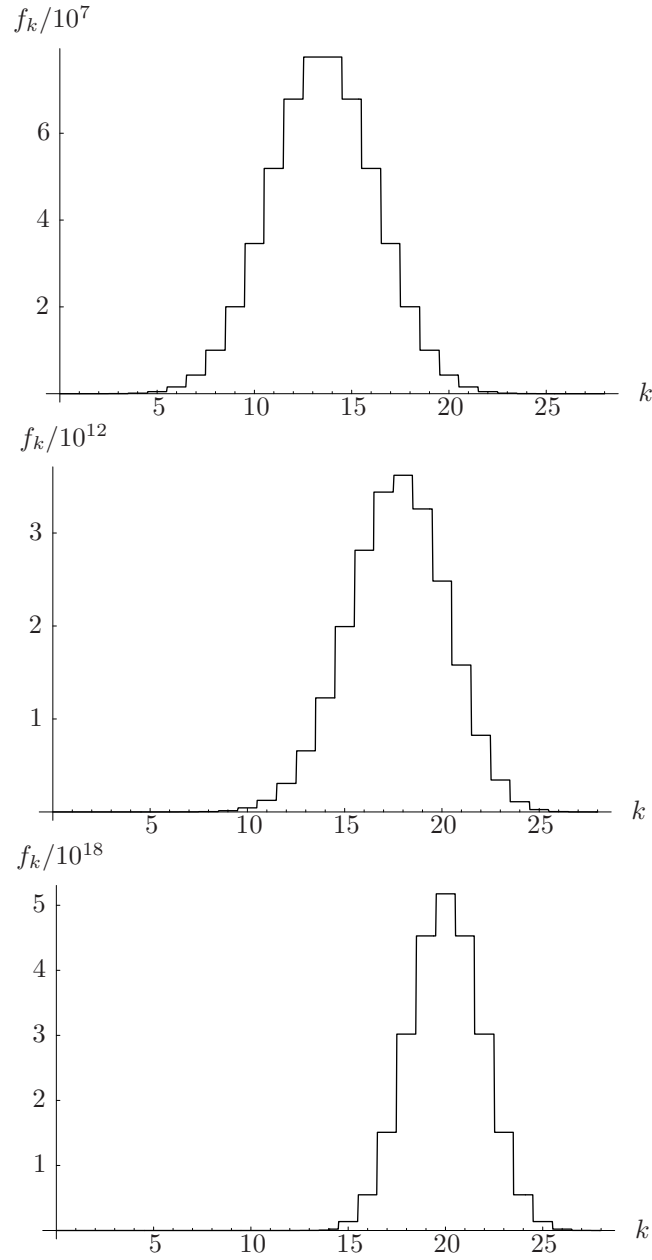


**Figure 2.2.** The  $f$ -vector shapes of the 28-dimensional simplex  $\Delta_{28}$ , the cross polytope  $C_{28}^*$ , and a cyclic polytope with 80 vertices  $C_{28}(80)$

$i_j$  arbitrarily, and also taking  $i_j + 1$  for  $k - \frac{d}{2}$  of these (see Figure 2.4). Thus, with a bit of an over-count, we get

$$f_{k-1}(C_d(n)) \begin{cases} = \binom{n}{k} & \text{for } k \leq \frac{d}{2}, \\ \sim \binom{n}{\frac{d}{2}} \binom{\frac{d}{2}}{k-\frac{d}{2}} & \text{for } k > \frac{d}{2}. \end{cases}$$

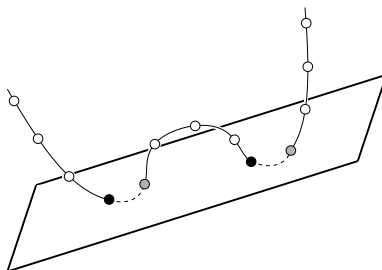


**Figure 2.3.** Sketch for Gale's evenness criterion.



**Figure 2.4.** An estimate for the number of facets of  $C_d(n)$ , for  $n \gg d$ , with  $d$  even: There are  $\binom{n}{d/2}$  choices for the black points; with high probability, they are non-adjacent; the  $\frac{d}{2}$  pairs can be completed by taking the gray points.

Clearly this peaks at  $x = \frac{3}{4}$ : We get the larger entries in the case  $k > \frac{d}{2}$ , and then the maximum is achieved when  $\binom{d/2}{k-d/2}$  is maximal, that is, for  $k = \frac{3}{4}d$ . Figure 2.2 gives a realistic impression of the  $f$ -vector shape of a cyclic polytope.

An explicit, exact formula for  $f_{k-1}(C_d(n))$  is available (Exercise 2.3), but this doesn't answer all the questions. In particular, is it really true that the  $f$ -vector is unimodal? As far as I know, the Unimodality Conjecture 2.1 has not been established in full for the cyclic polytopes. It does hold for small  $n > d$ , and certainly also if  $n \gg d$  is sufficiently large compared to  $d$  (with the  $f$ -vector peak at  $k = \lfloor \frac{3(d-1)}{4} \rfloor$ ), but in an intermediate range for  $n$  a challenge remains ...

### 2.3. Global constructions

We have seen classes of simplicial  $d$ -polytopes whose normalized  $f$ -vector functions  $\varphi(x) = f_{x(d-1)}$  peak at  $x = \frac{1}{2}$ , at  $x = \frac{2}{3}$ , or at  $x = \frac{3}{4}$ . By dualization we get simple polytopes with peaks at  $x = \frac{1}{3}$ , and at  $x = \frac{1}{4}$ . The "global constructions" of products and joins now yield examples with peaks in the whole range between  $x = \frac{1}{4}$  and  $x = \frac{3}{4}$ . (The product construction is elementary, well-known, and well-understood, but a review perhaps can't harm, also in view of our needs for Lecture 5. Joins are similarly elementary and well-understood, but perhaps not that well-known.)

**Example 2.7** (Products). Let  $P$  and  $Q$  be polytopes of dimensions  $d$  and  $e$ . Then the product

$$P \times Q := \{(x, y) : x \in P, y \in Q\}$$

is a polytope of dimension  $\dim(P \times Q) = \dim P + \dim Q = d + e$ .

The nonempty faces of  $P \times Q$  are the products of nonempty faces of  $P$  and nonempty faces of  $Q$ : In particular, the vertices of  $P \times Q$  are of the form “vertex times vertex,” the edges are of the form “edge times vertex” or “vertex times edge,” and the facets are “ $P$  times facet of  $Q$ ” or “facet of  $P$  times  $Q$ .” With the convention  $f_d(P) = f_e(Q) = 1$  this yields the formula

$$(2.1) \quad f_m(P \times Q) = \sum_{\substack{k+\ell=m \\ k, \ell \geq 0}} f_k(P) f_\ell(Q)$$

for  $m \geq 0$ .

The product construction is dual to the “free sum” construction,  $P \oplus Q$ : For this let  $x_0 \in P \subset \mathbb{R}^d$  and  $y_0 \in Q \subset \mathbb{R}^e$  be interior points, and take the convex hull

$$P \oplus Q := \text{conv}(P \times \{y_0\} \cup \{x_0\} \times Q).$$

The *proper* faces of  $P \oplus Q$  (that is, faces other than the polytope itself) arise as joins of proper faces of  $P$  and of  $Q$ .

The product and the free sum construction are illustrated in Figure 2.5.

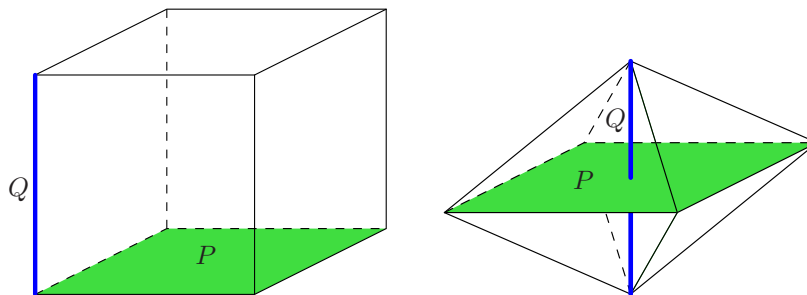


**Figure 2.5.** Product and free sum, for  $P = I^2$  and  $Q = I$

Since joins come up as faces of free sums, let’s briefly talk about joins.

**Example 2.8** (Joins). Let again  $P$  and  $Q$  be polytopes of dimensions  $d$  and  $e$ . Then the *join*  $P * Q$  is obtained by positioning  $P$  and  $Q$  into skew affine subspaces, and taking the convex hull. Thus the join is a polytope of dimension  $\dim(P * Q) = \dim P + \dim Q + 1 = d + e + 1$ .

The faces of  $P * Q$  are the joins of faces of  $P$  and faces of  $Q$ : This refers to *all* faces, including the empty face and the polytope itself. The corresponding formula, with  $f_{-1}(P) = f_{-1}(Q) = 1$ , is

$$(2.2) \quad f_m(P * Q) = \sum_{\substack{k+\ell=m-1 \\ k, \ell \geq -1}} f_k(P) f_\ell(Q),$$

valid for all  $m$ , that is, for  $-1 \leq m \leq d + e + 1$ .

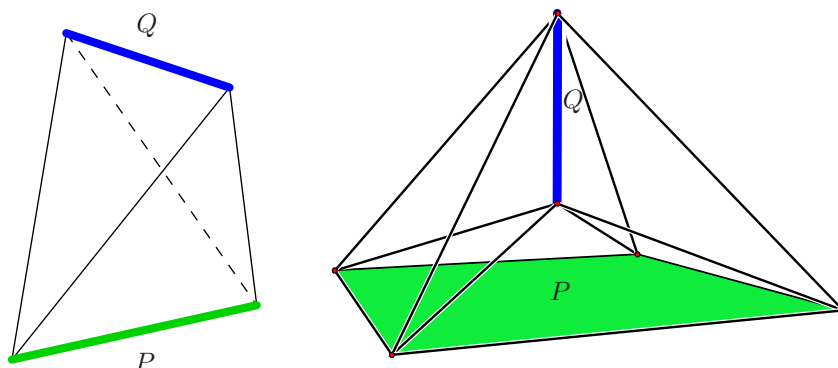


**Figure 2.6.** Joins  $I * I$  and  $I^2 * I$ , of an edge with an edge, resp. of a square with an edge

Joins are illustrated in Figure 2.6. The dual construction to taking joins is the join construction again.

Product and join are two distinct constructions, and they do yield different polytopes, of different dimensions (by 1). However, in a birds' eye view, asymptotically, they do behave quite similarly, and indeed, their effects on  $f$ -vector shapes are almost the same. Namely, the formulas (2.2) and (2.1) describe finite convolutions, and the only difference is whether the entry  $f_{-1} = 1$  is counted. For large dimensions, and large  $f$ -vectors, this does not make much of a difference, and in both cases we get a convolution of  $f$ -vector shapes. Thus, in particular, if the  $f$ -vectors of  $P$  and of  $Q$  have sharp peaks, then the product or join will have a peak as well:

$$(\text{peak at } x) * (\text{peak at } y) \longrightarrow (\text{peak at } \frac{d}{d+e}x + \frac{e}{d+e}y).$$

In particular, for  $d = e$  this yields

$$(\text{peak at } x) * (\text{peak at } y) \longrightarrow (\text{peak at } \frac{x+y}{2}).$$

To see this, just compute that if the peak (or, just the largest  $f$ -vector entry) for  $P_1$  is at  $x = \frac{k}{d}$  and for  $P_2$  at  $y = \frac{\ell}{e}$ , then the peak for  $P_1 * P_2$  will be at

$$\frac{k+\ell}{d+e} = \frac{k}{d} \frac{d}{d+e} + \frac{\ell}{e} \frac{e}{d+e} = x \frac{d}{d+e} + y \frac{e}{d+e}.$$

This also yields a convolution formula for the  $f$ -vector shape of  $P_1 \times P_2$  or  $P_1 * P_2$ , for large dimensions:

$$\varphi(x) = \int_0^1 \varphi_1\left(t \frac{d}{d+e}\right) \varphi_2\left((1-t) \frac{e}{d+e}\right) dt$$

Thus, by just taking products of sums of suitable cyclic polytopes and their duals, we do get polytopes with  $f$ -vector peaks in the whole range between  $\frac{1}{4}$  and  $\frac{3}{4}$ .

## 2.4. Local constructions

Perhaps the simplest local operation that can be applied to a polytope is to “stack a pyramid onto a simplicial facet.” To perform such a *stacking* operation geometrically, the new vertex of course has to be chosen carefully (*beyond* the simplicial facet, and *beneath* all other facets, in Grünbaum’s terminology [39, Sect. 5.2]), but

the combinatorial description is easy enough. In particular, we get the following  $f$ -vector equation:

$$f_k(\text{stack } P) = f_k(P) + f_k(\Delta_d) - f_k(\Delta_{d-1}).$$

This is valid for  $k < d - 1$ , the rest is “boundary effects” that we may safely ignore. Furthermore, the usual binomial recursion yields  $f_k(\Delta_d) - f_k(\Delta_{d-1}) = f_{k-1}(\Delta_{d-1})$ , and we get

$$f_k(\text{stack } P) = f_k(P) + f_{k-1}(\Delta_{d-1}).$$

So, the effect of stacking on the  $f$ -vector is to add a bump at  $x = \frac{1}{2}$ . The effect may be negligible if the  $f$ -vector of  $P$  is large, and has large slopes. However, any stacking operation destroys a simplicial facet and creates  $d$  new ones, so it can be repeated. We write  $\text{stack}^N P$  for a polytope that is obtained from  $P$  by  $N$  subsequent stacking operations. Thus we get

$$f_k(\text{stack}^N P) = f_k(P) + N f_{k-1}(\Delta_{d-1}),$$

where we may choose  $N \geq 0$  freely. Thus we are adding a function with peak at  $\frac{1}{2}$  to a function whose peak may be, for example, at  $\frac{2}{3}$ .

**Corollary 2.9** (Danzer 1964). *For large enough  $d$  and suitable  $N$ , the Unimodality Conjecture 2.1 fails for “ $N$ -fold stacked crosspolytopes”  $\text{stack}^N C_d^*$ .*

Indeed, Danzer apparently also derived that the  $f$ -vector of a simplicial  $d$ -polytope may have not only one dip (between two peaks), but arbitrarily many dips and peaks!

Also, dualization yields that a suitable number of vertex truncations applied to a high-dimensional cube leads to a simple polytope with a non-unimodal  $f$ -vector.

However, cross polytopes are not the most effective starting points for non-unimodal examples: If we use cyclic polytopes, then the peak (at  $\frac{3}{4}$ ) is further away from the peak for a simplex that we can “add” by stacking (at  $\frac{1}{2}$ ). Moreover, in cyclic polytopes we can control the number of vertices in fixed dimension as well, and thus make the peak at  $\frac{3}{4}$  as sharp as we want.

**Theorem 2.10** (Björner [13] [15], Lee [47] [12], Eckhoff [24]). *The Unimodality Conjecture 2.1 holds for simplicial  $d$ -polytopes of dimensions  $d \leq 19$ , but it fails for  $d \geq 20$ .*

Specifically: Stacking  $N = 259 \cdot 10^{11}$  times onto the cyclic polytope  $C_{20}(200)$ , one obtains a polytope with a dip  $f_{11} > f_{12} < f_{13}$  in the  $f$ -vector,

$$\begin{array}{rcl} f_{11} & = & 5049794068451336750 \\ & \vee & \\ f_{12} & = & 5043828885028647000 \\ & \wedge & \\ f_{13} & = & 5045792044986529500. \end{array}$$

The proof of the first part of Theorem 2.10 utilizes the  $g$ -theorem (see Stanley [69] and Björner [14]), which explicitly describes the  $f$ -vectors of the simplicial polytopes, plus a substantial amount of “binomial coefficient combinatorics.” See [15] for  $d \leq 16$ ; the extension to  $d \leq 19$ , due to Eckhoff, unfortunately is still not published.

If we leave the realm of simplicial polytopes, then it becomes even easier to construct polytopes with a non-unimodal  $f$ -vector. Then we can try to add the



$f$ -vectors of two polytopes with peaks at  $\frac{1}{4}$  and at  $\frac{3}{4}$ , say a cyclic polytope and its dual. And indeed, just as we can glue a pyramid onto a simplicial facet, we can glue any polytope with a simplicial facet onto another one — after a projective transformation, if needed [79, p. 274]. The  $f$ -vector effect of such a glueing is essentially

$$f(P\#P') = f(P) + f(P') - f(\Delta_{d-1});$$

if the  $f$ -vector components of  $P$  and of  $P'$  are large, then the simplex may be neglected, and we are essentially just “adding the  $f$ -vectors.”

We can even do this with cyclic polytopes: For example,  $C_d(n)$  is simplicial; its dual,  $C_d(n)^*$  is simple (without simplicial facets), but if we cut off (“truncate”) one of the simple vertices, then a simplicial facet results. Write  $C_d(n)'$  for the “dual with a vertex cut off.”

**Corollary 2.11** (Eckhoff [24]). *The Unimodality Conjecture 2.1 fails for  $d$ -polytopes of dimensions  $d \geq 8$ . In particular,*

$$f(C_8(25)\#C_8(25)') = (7149, 28800, 46800, 46400, 46400, 46800, 28800, 7149).$$

This  $f$ -vector has a nice “1% dip” in the middle! We don’t know whether the Unimodality Conjecture 2.1 is true for dimensions  $d = 6$  or  $7$ .

### Exercises

- 2.1. For  $d = 3, 4, 5, \dots$  construct a  $d$ -polytope with 12 vertices and 13 facets. How far do you get?
- 2.2. Show that  $f$ -vectors of 4-polytopes are unimodal.
- 2.3. Derive an *exact* formula for  $f_{d-1}(C_d(n))$ , and for  $f_k(C_d(n))$ , for even  $n$ .
- 2.4. Compute  $f_i(C_8(25))$ . How bad is the approximation given in Example 2.6?
- 2.5. Count and describe the 2-faces of a product of a pentagon and a heptagon,  $P_5 \times P_7$ .
- 2.6. Compute  $f((C_{10})^{10})$ , for the product of ten 10-gons. Where is the peak?
- 2.7. Estimate/compute  $d$  and  $N$  such that the “ $N$ -fold truncated  $d$ -cube” has a non-unimodal  $f$ -vector.
- 2.8. If you stack “too often” onto  $C_{20}(200)$ , then unimodality is restored. How often?



## LECTURE 3

### 2-Simple 2-Simplicial 4-Polytopes

The boundary complex of a 4-polytope is a 3-dimensional geometric structure. So, in contrast to the high-dimensional polytopes discussed in the previous lecture, we can hope to approach 4-polytopes via explicit visualization and geometric constructions. *Schlegel diagrams* are a key tool for this.\* Another one, which we will also depend on in a key moment of this lecture, is *dimensional analogy*: To describe a construction of 4-polytopes, we phrase a key step as a statement that it is valid “for all  $d \geq 3$ ,” where the visualization is done for the special case  $d = 3$ , while the most interesting results are obtained for  $d = 4$ .

The geometry and combinatorics of polytopes in dimension 4 is much more interesting, rich, and difficult than in 3 dimensions, because 4-polytopes aren’t constrained between only two extremes, simple and simplicial. Some of the most fascinating examples around, such as Schläfli’s 24-cell, are neither simple nor simplicial, but *2-simple 2-simplicial*. This property was thought to be rare until recently: Only a few years ago, exactly 8 such polytopes were known. (Unfortunately, a claim by Shephard from 1967 did not work out: In [39, p. 82] it had been claimed that Shephard could produce infinite families, and that each 4-dimensional convex body could be approximated by 2-simple 2-simplicial 4-polytopes, which would have established a conjecture by David Walkup. Compare [39, p. 96b])

The main goal for this lecture is to describe a simple, explicit, geometric construction that produces rich infinite families of 2-simple 2-simplicial 4-polytopes. The first infinite families, obtained by Eppstein, Kuperberg & Ziegler in 2001 [26], relied on rather subtle constructions, via Koebe–Thurston type edge-tangent realizations of 4-polytopes (which exist only in rare cases), and hyperbolic angle measurements. In contrast to this, the *deep vertex truncation* construction to be described here is remarkably simple; it appears in Paffenholz & Ziegler [57], while special instances (for semi-regular polytopes) can be traced back to Coxeter’s classic [22, Chap. VIII], who refers to Cesàro (1887) for the construction of the 24-cell by what we here call a “deep vertex truncation” of the regular 4-cube.

---

\*These were apparently introduced by Dr. Victor Schlegel, a highschool (Gymnasium) teacher from Waren an der Müritz, in his paper [67] from 1883. The plates for the paper include a Schlegel diagram (“Zellgewebe”) of a 4-cube, as well as two quite insufficient drawings representing the 24-cell. Classical, beautiful drawing may be found in Hilbert & Cohn-Vossen [41, p. 135].

### 3.1. Examples

Let's start with examples of well-known 4-polytopes — and for each of those let's look at a Schlegel diagram, and record the  $f$ -vector

$$(f_0, f_1, f_2, f_3) = (\# \text{ vertices, } \# \text{ edges, } \# \text{ 2-faces (= ridges), } \# \text{ facets}).$$

A *Schlegel diagram* is a way to visualize a 4-polytope in terms of a 3-dimensional complex. We can't develop the theory of Schlegel diagrams here (see [39, Sect. 3.3] and [79, Lect. 5]), but we can offer two interpretations, both in terms of dimensional analogy.

- Assume that one face of a 3-polytope is transparent (a “window”), press your nose to the window, and look inside: Then you will see all the other faces of the polytope through the window. If you now close one eye (and thus lose the spatial impression, or depth view), then you will see how the other faces tile the window; you can see how they fit together, and thus the whole combinatorial structure of the 3-polytope is projected into a 2-dimensional window. This is the Schlegel diagram of a 3-polytope.
- Any 3-polytope can be projectively deformed in such a way that looking at it from a suitable point, you *see* all faces except for one single face, which is on the back. What you see is a polytopal complex which has the same shape as the back face, but this is broken into all the many faces that you see on the front side. What you see is the 2-dimensional Schlegel diagram of a 3-polytope.

The Schlegel diagram of a 4-polytope, analogously, is a 3-dimensional complex that represents all the faces of the polytope, except for one facet (the window resp. back facet). The whole combinatorial structure of the polytope may be read from such a visualization. Thus, for example, one can tell whether the polytope is simple, or simplicial, or cubical, etc.

The pictures of Schlegel diagrams as presented in the following are generated automatically in the `polymake` system by Gawilow & Joswig [31], with the `javaview` back-end by Polthier et al. [58]. They have three limitations: They show only a 2-dimensional projection of an object that you should see rotating, 3-dimensionally, on a screen; they depict only the edges, so in some examples it is hard to tell/imagine where the faces and facet-boundaries go; and we don't have color available here. Nevertheless, I think they are impressive, and you should be able to “see” in them what the (boundary complexes of) some 4-polytopes look like.

**Example 3.1** (Simplex, cube, and cross polytope). Schlegel diagrams of the 4-simplex, the 4-cube and the 4-dimensional cross polytope appear in Figure 3.1. You should read off the  $f$ -vectors from this figure:  $f(\Delta_4) = (5, 10, 10, 5)$ ,  $f(C_4) = (16, 32, 24, 8)$ , and  $f(C_4^*) = (8, 24, 32, 16)$ .

The simplex and cube are simple, so  $f_1 = 2f_0$ , while the simplex and cross polytope are simplicial, so  $f_2 = 2f_3$ .

**Example 3.2** (A cubical 4-polytope with the graph of a 5-cube [43]). The construction

$$P := \text{conv}((2Q \times Q) \cup (Q \times 2Q)),$$

for a square such as  $Q = [-1, 1]^2$ , yields a 4-polytope whose Schlegel diagram is displayed in Figure 3.2. This polytope is *cubical*: All its facets are combinatorially equivalent to the 3-cube  $[-1, 1]^3$ .

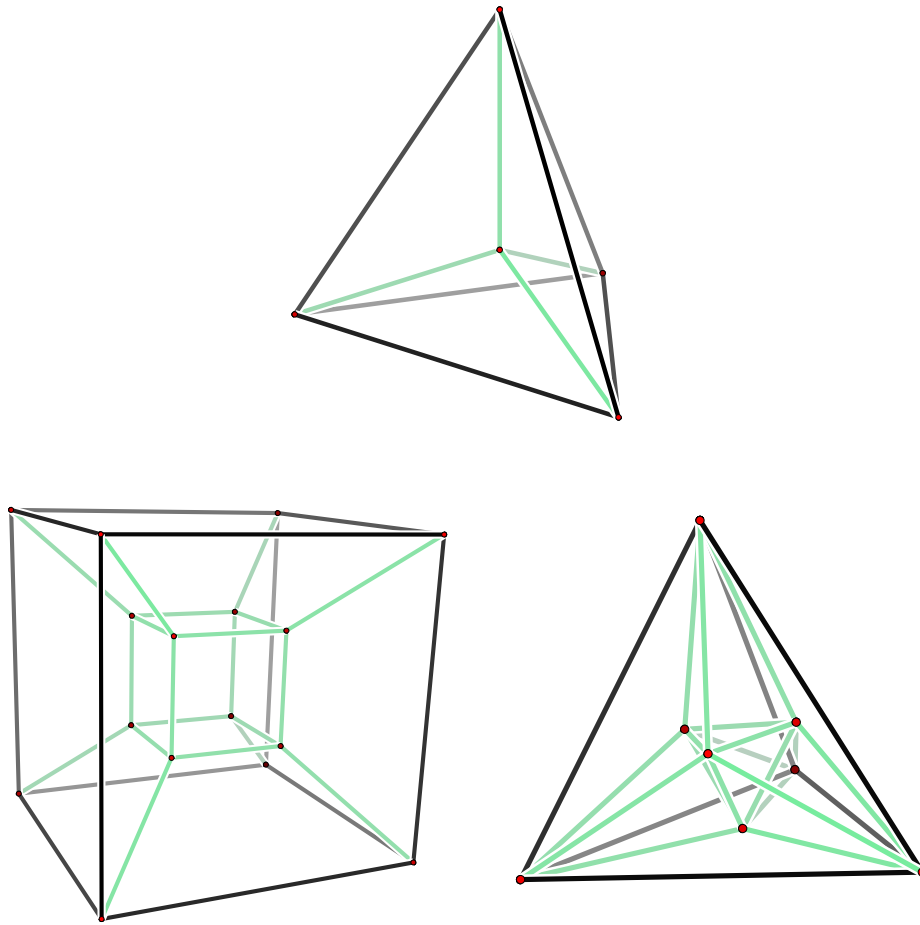


**Figure 3.1.** Schlegel diagrams for the 4-dimensional simplex, cube, and cross polytope

The  $f$ -vector  $(32, 80, 72, 24)$  may be derived from the figure, but indeed it may also be deduced just from the information that this is a cubical 4-polytope with the graph of a 5-cube. (The latter yields  $f_0$  and  $f_1$ , the “cubical” property implies  $2f_2 = 6f_3$  by double counting, and then there is the Euler–Poincaré equation [79, Sect. 8.2], which for 4-polytopes reads  $f_0 - f_1 + f_2 - f_3 = 0$ . See also Exercise 3.2.)

**Example 3.3** (The hypersimplex). The hypersimplexes form a 2-parameter family  $\Delta_{d-1}(k)$  of remarkable polytopes; as Robert MacPherson said in his PCMI lectures, they have by far not received the attention, study, and popularity that they deserve. They do appear, for example, as  $K_k^d$  in [39, p.65], as  $\Delta^{k,\ell}$  in [29, Sect. 1.6] (where apparently the name “hypersimplex” appeared first), in [35], in [34, p. 207], and in [23]; but also elsewhere they appear under disguise, for example, as the cycle polytopes of uniform matroids (see e.g. [38]).

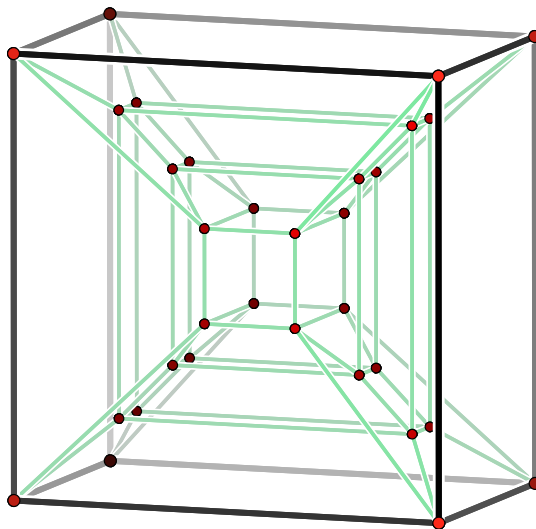


**Figure 3.2.** A cubical 4-polytope with the graph of the 5-cube

The hypersimplex  $\Delta_{d-1}(k)$  may be defined as the convex hull of all the 0/1-vectors of length  $d$  that consist of  $k$  ones and  $d - k$  zeroes. This is a  $(d - 1)$ -dimensional polytope with  $\binom{d}{k}$  vertices. In the special case  $k = 1$  and  $k = d - 1$  we obtain simplices.

What we call *the hypersimplex* is a 4-dimensional polytope  $\Delta_4(2)$  that appears in this family. It may be defined, lying on a hyperplane in  $\mathbb{R}^5$ , as

$$\{x \in [0, 1]^5 : \sum_{i=1}^5 x_i = 2\} = \text{conv}\{e_i + e_j : 1 \leq i < j \leq 5\},$$

or equivalently, after projection to  $\mathbb{R}^4$  by “deleting the last coordinate,” as

$$\{x \in [0, 1]^4 : 1 \leq \sum_{i=1}^4 x_i \leq 2\} = \text{conv}(\{e_i : 1 \leq i \leq 4\} \cup \{e_i + e_j : 1 \leq i < j \leq 4\}).$$

The first representation is more symmetric: It yields “by inspection” that all  $\binom{5}{2} = 10$  vertices of this polytope are equivalent (under symmetries that permute the coordinates), but that there are two types of facets, five simplices and five octahedra, which appear in vertex-disjoint pairs, “opposite to each other,” in parallel hyperplanes. In particular, all the facets are simplicial, that is, all the 2-faces are triangles, so the polytope is *2-simplicial*.

The second representation has the advantage of being full-dimensional, and it supplies us with a Schlegel diagram (using an octahedron facet as a “window”), as displayed in Figure 3.3. In the figure we may see that the (ten, equivalent) vertex figures are triangular prisms, so they are simple; thus in this 4-polytope, each edge is in exactly three facets, so the polytope is *2-simple*. So we have seen our first example (other than the 4-simplex) of a 2-simple, 2-simplicial 4-polytope.

From the data given it is easy to compute the  $f$ -vector of the hypersimplex: It is  $f = (10, 30, 30, 10)$ .

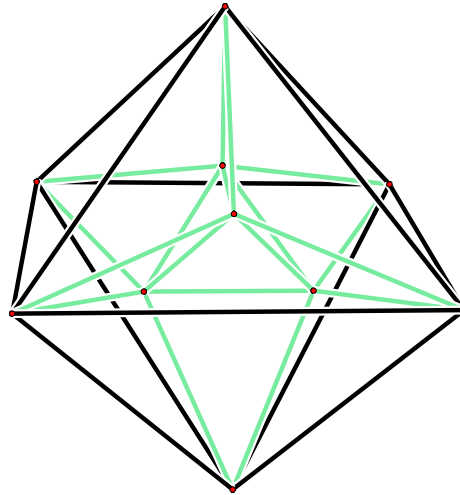


Figure 3.3. A Schlegel diagram of the hypersimplex

### 3.2. 2-simple 2-simplicial 4-polytopes

**Definition 3.4.** A 4-polytope  $P \subseteq \mathbb{R}^4$  is *2-simple 2-simplicial* (“2s2s” for short) if all 2-faces of  $P$ , and of  $P^*$ , are triangles.

The definition given here has the nice feature of being self-dual: Clearly,  $P$  is 2s2s if and only if its dual  $P^*$  is 2s2s. A more explicit version is that a 4-polytope is 2s2s if and only if

- every 2-face has the minimal number 3 of vertices, and if
- every 1-face (edge) lies in the minimal number 3 of facets.

Still equivalently, this is if and only if

- for every 2-face  $G$  the lower interval  $[\emptyset, G]$  in the face lattice of  $P$  is boolean, and if
- for every 1-face  $e$  the upper interval  $[e, P]$  in the face lattice of  $P$  is boolean.

Thus the 2s2s property may be pictured in analogy with the properties of being simple, or being simplicial. For this we note that, for example,  $P$  is simplicial if

- for every 3-face  $F$  (facet) the lower interval  $[\emptyset, F]$  in the face lattice of  $P$  is boolean, and if
- for every 2-face  $R$  (ridge) the upper interval  $[R, P]$  in the face lattice of  $P$  is boolean.

(The first property just says that the facets should be simplices; the second property is automatically satisfied: Every ridge lies in two facets.) And similarly for simple 4-polytopes — see Figure 3.4.

Of course all this suggests generalizations, to ask for  *$h$ -simple  $k$ -simplicial  $d$ -polytopes*, apparently introduced by Grünbaum [39, Sect. 4.5]. For  $h + k > d$  these

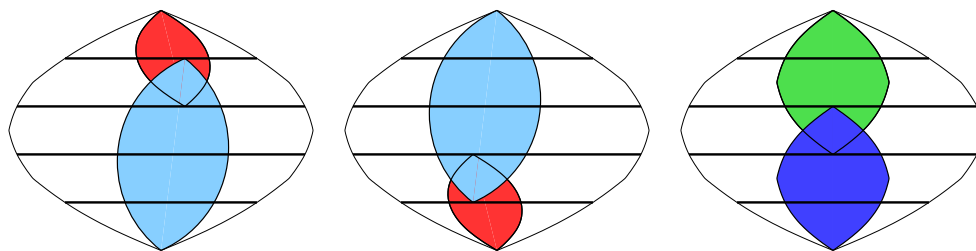


**Figure 3.4.** Simplicial, simple, and 2s2s 4-polytopes in terms of their face lattices: The shaded intervals, and all the other intervals between the same rank levels, must be boolean.

don't exist (other than the  $d$ -simplex), but also for small  $h$  and  $k$  they are hard to construct. Indeed, are there any 5-simple 5-simplicial  $d$ -polytopes that are not simplexes? Not a single example is known. Compare [57] for more information. Here we will restrict ourselves to the 4-dimensional case of 2s2s polytopes. Let's note one interesting property that is specific for the 4-dimensional case, and which also confirms the impression that 2s2s 4-polytopes form a “diagonal” case.

**Lemma 3.5.** *Every 2s2s 4-polytope has a symmetric  $f$ -vector:  $f_0 = f_3$ ,  $f_1 = f_2$ .*

**Proof.** If  $P$  is 2-simplicial, then each 2-face has three edges. Thus the number of incidences between 2-faces and edges, denoted  $f_{12}$ , is  $f_{12} = 3f_2$ . If it is 2-simple, then each edge lies in three 2-faces, that is, the number of incidences is  $f_{12} = 3f_1$ . Combination of the two conditions forces  $f_1 = f_2$ . With this, Euler's equation yields  $f_0 = f_3$ .  $\square$

This proof may be rephrased in terms of the face lattice: For 4-polytopes the 2s2s conditions force the two middle rank levels of the face lattice to form a bipartite cubic graph — which as any other regular bipartite graph has to have the same number of vertices on each shore. You should identify this bipartite cubical graph in the face lattice of the hypersimplex, as displayed in Figure 3.5, and thus verify the 2s2s property for this face lattice. The symmetry of the  $f$ -vector  $(10, 30, 30, 10)$  is explained by Lemma 3.5; nevertheless, the hypersimplex and its face lattice are not self-dual: There are two types of facets, but only one symmetry class of vertices.

The fact that the dual of any 2s2s 4-polytope is again 2s2s (by definition), and the symmetry property for the  $f$ -vector, might suggest that 2s2s polytopes live in some sense “between” simple and simplicial. This is not true, as we will see in the next lecture, when we locate their  $f$ -vectors in the cone of all  $f$ -vectors of 4-polytopes. Indeed, the 2s2s polytopes are so interesting because they form a class of extremal polytopes in terms of the flag vector: A 4-polytope is 2s2s if and only if the valid inequality

$$2f_{03} \geq (f_1 + f_2) + 2(f_0 + f_3)$$

holds with equality. (Compare Exercise 3.7.)



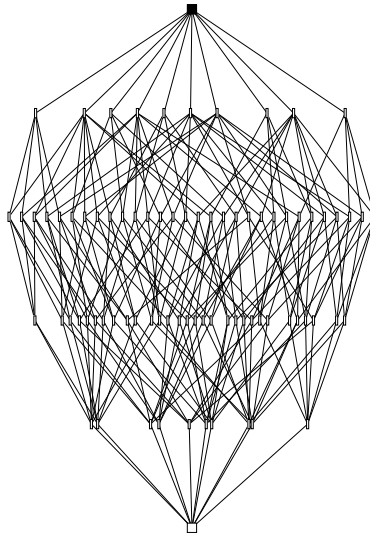


**Figure 3.5.** The face lattice of the hypersimplex

### 3.3. Deep vertex truncation

The idea for “deep vertex truncation” is very easy: Cut off all vertices of a polytope — but don’t just truncate the vertices, but cut them off by “deep cuts,” that is, so deeply that exactly one point remains from each edge.

All that is said and done about “deep vertex truncation” in the following works and makes sense for  $d \geq 3$ . Nevertheless, the pictures will primarily represent the case  $d = 3$ , while the most interesting results appear for  $d = 4$ .

**Definition 3.6** (Deep vertex truncation). Let  $P$  be a  $d$ -polytope,  $d \geq 2$ .

A *deep vertex truncation*

$$\text{DVT}(P) = P \cap \bigcap_{v \in V(P)} H_v^-$$

of  $P$  is obtained by cutting off all the vertices  $v \in V(P)$  of  $P$  (by closed halfspaces  $H_v^-$ , one for each vertex  $v$ ) in such a way that from each edge  $e$  of  $P$ , exactly one (relative interior) point  $p_e$  remains.

Equivalently, a deep vertex truncation is obtained as the convex hull

$$\text{DVT}(P) = \text{conv} \{p_e : e \in E(P)\}$$

of points  $p_e$  placed on the edges  $e \in E(P)$  of  $P$  in such a way that for each vertex of  $P$ , the points  $p_e$  chosen on the edges adjacent to  $v$  lie on a hyperplane  $H_v$ .

It is quite obvious that a deep vertex truncation  $\text{DVT}(P)$  can be constructed for each simple polytope  $P$ , but we will be particularly interested in the case of simplicial polytopes: For these it is not so clear that the cutting can be performed so that all constraints are satisfied simultaneously.

**Lemma 3.7.** *Every 3-polytope has a realization for which deep vertex truncation can be performed.*

**Proof.** Take an edge-tangent Koebe–Andreev–Thurston representation (according to Lecture 1). Then  $p_e$  can be taken as the tangency points, and the cutting hyperplanes  $H_v$  are spanned by the vertex horizon circles.  $\square$

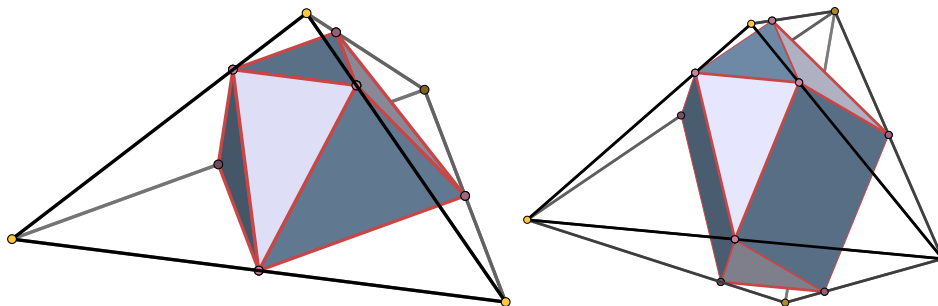


**Figure 3.6.** Deep vertex truncation of a simplex and of a bipyramid yields an octahedron, and a polytope that is “glued” from two octahedra. (Pictures from [57])

For  $d \geq 3$ , every deep vertex truncation polytope  $\text{DVT}(P)$  has two types of facets:

- deep vertex truncations  $\text{DVT}(F)$  of the facets  $F$  of  $P$ , and
- the vertex figures  $P \cap H_v = \text{conv}\{p_e : e \ni v\}$  of  $P$ .

**Proposition 3.8** (Paffenholz & Ziegler [57]). *If  $P$  is a simplicial 4-polytope, then any deep vertex truncation  $\text{DVT}(P)$  is 2-simple and 2-simplicial.*

**Proof.** The two types of facets of  $\text{DVT}(P)$  are the octahedra  $\text{DVT}(F)$ , for the tetrahedron facets  $F$  of  $P$ , and the vertex figures of  $P$ , which are simplicial. Thus  $\text{DVT}(P)$  is 2-simplicial.

Since all edges of  $P$  are reduced to points by deep vertex truncation, all the edges of  $\text{DVT}(P)$  are “new,” they arise by deep vertex truncation from the 2-faces (that is, the ridges) of  $P$ . Each such ridge lies in two facets  $F_1, F_2$  of  $P$ , so the edge we are looking at lies in two facets  $\text{DVT}(F_1)$  and  $\text{DVT}(F_2)$  of the first type, and in one facet of the second type. Thus each edge of  $\text{DVT}(P)$  lies in exactly three facets, that is,  $\text{DVT}(P)$  is 2-simple.  $\square$

So we have that  $\text{DVT}(P)$  is 2s2s for any simplicial 4-polytope  $P \dots$  if it exists. And that’s the problem: In general it is not at all guaranteed that deep vertex truncation can be performed. One would try to realize cyclic 4-polytopes in such a way that deep vertex truncations can be performed, but it seems that this is not possible. Similarly, if a sum  $P_m \oplus P_n$  is realized “the obvious way,” with regular polygons in orthogonal subspaces, then deep vertex truncation is not possible except for very special cases (such as  $\frac{1}{m} + \frac{1}{n} \geq \frac{1}{2}$ ): It is quite surprising that the sums of polygons *do* have a realization such that deep vertex truncation is possible, as proved by Paffenholz [55]. On the other hand, there does not seem to be a single example of a simplicial polytope for which it has been *proved* that deep vertex truncation is impossible for all realizations.

However, in special cases deep vertex truncation can indeed be performed. In particular, any *regular* polytope admits a deep vertex truncation — just take the

edge midpoints for  $p_e$ . From this we get the following three examples of 2s2s 4-polytopes:

- Deep vertex truncation of a simplex,  $\text{DVT}(\Delta_4)$ , yields the hypersimplex.
- Deep vertex truncation of the 4-dimensional cross polytope,

$$C_4^* = \text{conv}\{\pm e_i : 1 \leq i \leq 4\} = \{x \in \mathbb{R}^4 : |x_1| + |x_2| + |x_3| + |x_4| \leq 1\},$$

yields Schläfli's 24-cell (see Figure 3.7):

$$\begin{aligned} \text{DVT}(C_4^*) &= \text{conv}\{\pm \frac{1}{2}e_i \pm \frac{1}{2}e_j : 1 \leq i < j \leq 4\} \\ &= \{x \in \mathbb{R}^4 : |x_i| \leq 1 \text{ for } 1 \leq i \leq 4, |x_1| + |x_2| + |x_3| + |x_4| \leq 1\}. \end{aligned}$$

- Deep vertex truncation of the regular 600-cell (which has 600 regular tetrahedra as facets) yields a 2s2s 4-polytope with 720 vertices, whose vertex figures are prisms over regular pentagons; its facets are 600 octahedra, and 120 regular icosahedra. It seems that this remarkable polytope, with  $f$ -vector  $(720, 3600, 3600, 720)$ , first occurred in the literature in 1994, as the dual of the “dipyramidal 720-cell” constructed by Gévay [36]. See also Exercise 3.2.

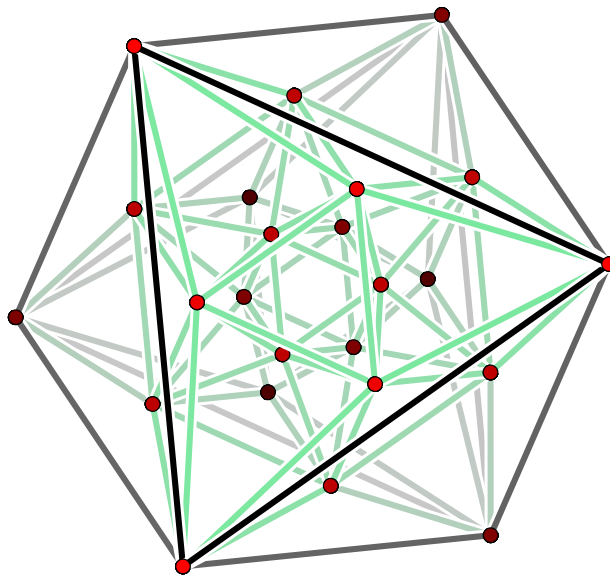


Figure 3.7. The 24-cell

### 3.4. Constructing $\text{DVT}(\text{Stack}(n, 4))$

The stacked polytopes form an infinite family of simplicial polytopes which can quite easily be realized in such a way that deep vertex truncation can be performed.

For this, we denote by  $\text{Stack}(n, d) := \text{stack}^n(\Delta_d)$  any combinatorial type of a  $d$ -polytope,  $d \geq 3$ , which is obtained by  $n$  times stacking a pyramid onto a simplex facet, starting at a  $d$ -simplex. This is a simplicial  $d$ -polytope with  $d + 1 + n$  vertices and  $d + 1 + n(d - 1)$  facets; see Exercise 3.3. Note that the notation “ $\text{Stack}(n, d)$ ” does not specify a combinatorial type; many different types may be obtained by stacking onto different sequences of facets (cf. Exercise 3.6).

**Theorem 3.9** (Paffenholz & Ziegler [57]). *Any combinatorial type of a stacked  $d$ -polytope  $\text{Stack}(n, d)$  can be realized so that it admits a deep vertex truncation.*

**Proof.** We proceed by induction on  $n$ , starting at  $n = 0$ , with a  $d$ -simplex, and a deep vertex truncation that takes the convex hull of the edge midpoints.

Assume now that  $\text{Stack}(n, d)$  has been realized as  $P \subset \mathbb{R}^d$  such that  $\text{DVT}(P)$  can be obtained by a suitable choice of points  $p_e$  on the edges  $e \subset P$ . Assume that  $\text{Stack}(n + 1, d)$  arises by stacking onto a facet of  $\text{Stack}(n, d)$  that is realized by the facet  $F \subset P$  with vertex set  $\{v_1, \dots, v_d\}$ . The “new” vertex  $w$  is now chosen “beyond” the facet  $\text{DVT}(F)$  of  $\text{DVT}(P)$ , and “beneath” all other facets of  $\text{DVT}(P)$ . That is, addition of  $w$  to  $\text{DVT}(P)$  would mean stacking a pyramid onto the facet  $\text{DVT}(F)$  of  $\text{DVT}(P)$ . In particular,  $w$  lies “beyond” the facet  $F$  of  $P$ , and “beneath” all other facets of  $P$ , so  $P' := \text{conv}(\{w\} \cup P)$  is a stacked polytope realizing  $\text{Stack}(n + 1, d)$ , as required.

The facet hyperplanes  $H_{v_i}$  of  $\text{DVT}(P)$  cut the edges  $[v_i, w]$  of  $P'$  in points  $p_i$ : This is since  $w$  is beneath  $H_{v_i}$ , while  $v_i$  is cut off by  $H_{v_i}$ . Thus we obtain points  $p_i$  on the new edges of  $P'$ , and the hyperplane  $H_w := \text{aff}\{p_1, \dots, p_d\}$  may be taken to cut off the new vertex  $w$  of  $P'$ . This new truncation plane is determined uniquely by the  $d$  intersection points, because the new vertex  $w$  of  $P'$  is simple.  $\square$

This theorem is valid for all  $d \geq 3$ ; in particular, 3D-pictures work. (Figure 3.8 is a feeble attempt.) However, the construction produces by far the most interesting results for  $d = 4$ .

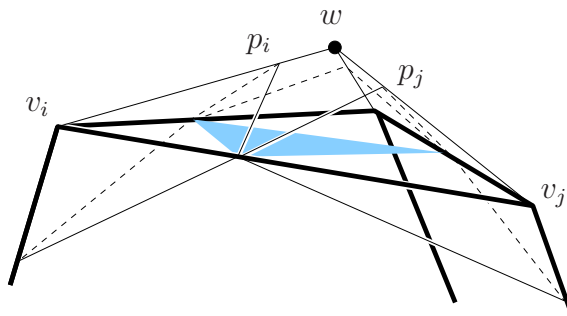


**Figure 3.8.** The induction step in Theorem 3.9, for  $d = 3$ .  $\text{DVT}(F)$  is drawn shaded.

**Corollary 3.10** ([57]). *For each  $n \geq 0$ , and for every type of stacked 4-polytope  $\text{Stack}(n, 4)$  with  $f$ -vector  $(5 + n, 10 + 4n, 10 + 6n, 5 + 3n)$ , there is a corresponding 2-simple 2-simplicial 4-polytope  $\text{DVT}(\text{Stack}(n, 4))$ , with  $f$ -vector*

$$f(\text{DVT}(\text{Stack}(n, 4))) = (10 + 4n, 30 + 18n, 30 + 18n, 10 + 4n).$$

In particular, this yields infinitely many combinatorial types of 2-simple 2-simplicial 4-polytopes. Moreover, with a bit of care the proof of Theorem 3.9 yields these polytopes with rational vertex coordinates. See [54] for explicit examples of such coordinates.

**Corollary 3.11** ([57]). *The number of combinatorial types of 2-simple 2-simplicial 4-polytopes with  $10 + 4n$  vertices grows exponentially in  $n$ .*

See Paffenholz & Werner [56] for further constructions of 2-simple 2-simplicial 4-polytopes with interesting  $f$ -vectors. In particular, they describe the “smallest” example of such a polytope (other than the simplex), which has only 9 vertices.

### Exercises

- 3.1. Show that any simple or simplicial  $d$ -polytope with  $f_0 = f_{d-1}$  must be a simplex, or 2-dimensional.
- 3.2. Compute the full  $f$ -vectors, as well as the number  $f_{03}$  of vertex-facet incidences, for the following 4-polytopes, based only on the information given here:
  - (a) The 24-cell: a 2s2s polytope whose facets are 24 octahedra;
  - (b) The 600-cell: a simple polytope whose facets are 120 dodecahedra;
  - (c) The 720-cell: a 2s2s 4-polytope whose facets are 720 bipyramids over pentagons;
  - (d) A neighborly cubical polytope  $\text{NCP}_4^n$ , a cubical polytope with the graph of the  $n$ -cube ( $n \geq 4$ ).
- 3.3. Compute the full  $f$ -vectors of the stacked  $d$ -polytopes  $\text{Stack}(n, d)$ .
- 3.4. Show that if a 4-polytope  $P$  is not simplicial, then  $\text{DVT}(P)$  cannot be 2-simplicial.
- 3.5. Find coordinates for  $\text{DVT}(\text{Stack}(1, 4))$ . Check them with `polymake`. (This is Braden’s “glued hypersimplex” [18].)
- 3.6. Show that there are exponentially many distinct combinatorial types of stacked  $d$ -polytopes with  $d + 1 + n$  vertices, for any  $d \geq 3$ . Derive that there are exponentially many types of 2-simple 2-simplicial 4-polytopes with the same  $f$ -vector.
- 3.7. Show that  $f_{13} = f_{03} + 2f_2 - 2f_3$ , and dually  $f_{02} = f_{03} + 2f_1 - 2f_0$ , holds for the flag vector of each 4-polytope. (Hint: Sum the Euler equations for the facets, which are 3-polytopes.) Derive from this that the inequality  $2f_{03} \geq (f_1 + f_2) + 2(f_0 + f_3)$  is valid for all 4-polytopes, and that it is tight exactly for the 2-simple 2-simplicial 4-polytopes.
- 3.8. Show that there is no  $f$ -vector inequality (not involving  $f_{03}$ ) that characterizes the 2s2s 4-polytopes.
- 3.9. If  $P$  is a  $d$ -dimensional simplicial polytope, and if  $\text{DVT}(P)$  exists, is  $\text{DVT}(P)$  then 2-simple? 2-simplicial?



## LECTURE 4

### *f*-Vectors of 4-Polytopes

The *f*-vector of a 4-polytope is a quadruple of integers  $f(P) = (f_0, f_1, f_2, f_3)$ , but due to the Euler-Poincaré relation the set of all *f*-vectors of 4-polytopes is a 3-dimensional set: It lies on the “Euler-Poincaré hyperplane” in  $\mathbb{R}^4$ , given by

$$f_0 - f_1 + f_2 - f_3 = 0.$$

The task we are facing is to describe the set of all *f*-vectors,

$$\mathcal{F}_4 := \{f(P) = (f_0, f_1, f_2, f_3) \in \mathbb{Z}^4 : P \text{ a convex 4-polytope}\}.$$

Here “describe” may mean a number of different things: Probably one should not hope for a complete description (as Steinitz got for the 3-dimensional case), since the set of *f*-vectors is way more complicated in the 4-dimensional case.

Indeed,  $\mathcal{F}_4$  is *not* the set of all integral points in a polyhedral cone, or even in a convex set. This may be seen from the characterizations of the projections of  $\mathcal{F}_4$  to the coordinate 2-planes in  $\mathbb{R}^4$ , by Grünbaum, Barnette, and Reay [39, Sect. 10.4] [8] [10], which show non-convexities and holes (see Figure 4.1). Or you just note that some of the rather basic, tight inequalities, such as the upper bound inequality  $f_1 \leq \binom{f_0}{2}$ , are concave. For example,

$$\begin{aligned} f(C_4(5)) &= (5, 10, 10, 5), \\ f(C_4(7)) &= (7, 21, 28, 14), \\ f(C_4(9)) &= (9, 36, 54, 27). \end{aligned}$$

The midpoint of the segment between  $f(C_4(5))$  and  $f(C_4(9))$  is the integral point  $(7, 23, 32, 16)$ : It violates the upper bound inequality, and indeed a 4-polytope with 7 vertices cannot contain more than the  $21 = \binom{7}{2} = f_1(C_4(7))$  edges. (See also Bayer [11], Höppner & Ziegler [42].)

In the following, we will head for a complete description of the *f*-vector cone for 4-polytopes,  $\text{cone}(\mathcal{F}_4)$ . This seems to be a challenging but realistic goal. Once that is achieved (the “2006 project”), a logical next goal might be a description of the “large” *f*-vectors, that is, of

$$\{f(P) = (f_0, f_1, f_2, f_3) \in \mathbb{Z}^4 : P \text{ a convex 4-polytope, } f_0 + f_3 \geq M\}$$

for some large  $M$ . But let’s not get too ambitious too fast.

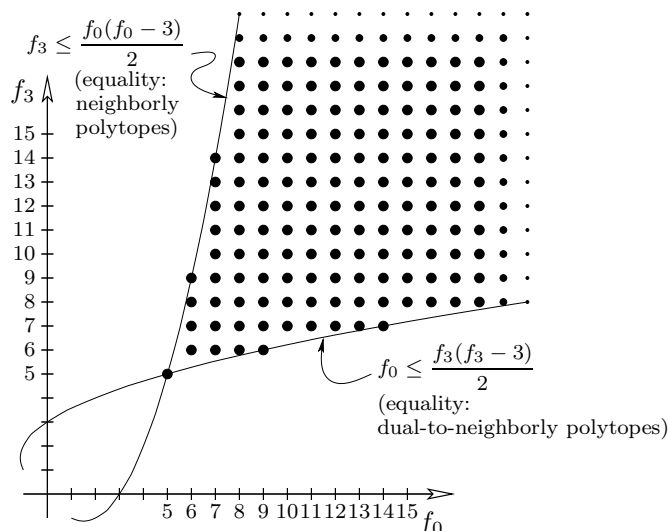


**Figure 4.1.** The  $(f_0, f_3)$ -pairs of convex 4-polytopes, according to Grünbaum [39, Sect. 10.4]

#### 4.1. The $f$ -vector cone

**Definition 4.1** ( $f$ -vector cone). The  $f$ -vector cone of 4-polytopes,  $\text{cone}(\mathcal{F}_4)$ , is the topological closure of the convex cone with apex  $f(\Delta_4) = (5, 10, 10, 5)$  that is spanned by the  $f$ -vectors of 4-polytopes,

$$\left\{ f(\Delta_4) + \sum_{i=1}^N \lambda_i (f(P_i) - f(\Delta_4)) : P_1, \dots, P_N \text{ 4-polytopes, } \lambda_1, \dots, \lambda_N \geq 0 \right\}.$$

Equivalently,  $\text{cone}(\mathcal{F}_4) \subset \mathbb{R}^4$  is the solution set to all the linear inequalities that are valid for all  $f$ -vectors for 4-polytopes, and that are tight at the  $f$ -vector of the simplex.

The equivalence between the two versions of the definition rests on basic facts about closed convex sets, which you should put together yourself (Exercise 4.1). You are also asked to verify that the cone generated by the  $f$ -vectors is not closed, so we do have to take the topological closure (Exercise 4.2).

The closed convex cone we are looking at is 3-dimensional, so we may view it as the cone over a 2-dimensional convex figure, which might be just a pentagon or hexagon. Instead of looking at a 2-dimensional section (say intersecting by  $f_1 + f_2 = 100$ ), we may equivalently introduce homogeneous (“projective”) coordinates, which are rational linear functions, normalized to yield “ $\frac{0}{0}$ ” at the  $f$ -vector of a simplex (compare Lecture 1). There is no unique best way to do this; we choose

$$\varphi_0 := \frac{f_0 - 5}{f_1 + f_2 - 20} \quad \text{and} \quad \varphi_3 := \frac{f_3 - 5}{f_1 + f_2 - 20}$$

as our homogeneous coordinates. (Figure 4.2 illustrates the geometry of such a rational function on a cone.) So we are trying to describe  $\text{proj}(\mathcal{F}_4) \subset \mathbb{R}^2$ , the closure of

$$\text{conv}\{(\varphi_0(P), \varphi_3(P)) \in \mathbb{R}^2 : P \text{ a convex 4-polytope}\}.$$



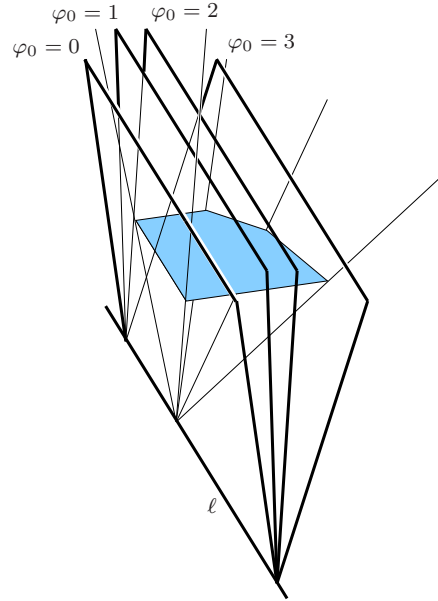


**Figure 4.2.** The function  $\varphi_0$  is constant on certain planes that contain the apex of the cone. It is not defined on the line  $\ell$  where all those planes intersect. (In terms of  $(f_0, f_1, f_2)$ -coordinates,  $\ell$  is defined by  $f_0 = 5$  and  $f_1 + f_2 = 20$ .)

Any 4-polytope yields a (rational) point in the  $(\varphi_0, \varphi_3)$ -plane. Any valid linear inequality, tight at the 4-simplex, translates into a linear inequality in  $\varphi_0$  and  $\varphi_3$ . So let's look at some families of polytopes and of linear inequalities that we know, and let's see what they buy us.

#### Some 4-polytopes we know:

$$\begin{array}{llll}
 \text{Stacked:} & (5 + n, 10 + 4n, 10 + 6n, 5 + 3n) & \longrightarrow & \left(\frac{1}{10}, \frac{3}{10}\right) \\
 \text{Truncated:} & (5 + 3n, 10 + 6n, 10 + 4n, 5 + n) & \longrightarrow & \left(\frac{3}{10}, \frac{1}{10}\right) \\
 \text{Cyclic:} & \left(n, \frac{n(n-1)}{2}, n(n-3), \frac{n(n-3)}{2}\right) & \xrightarrow{n \rightarrow \infty} & \left(0, \frac{1}{3}\right) \\
 \text{Dual-to-cyclic:} & \left(\frac{n(n-3)}{2}, n(n-3), \frac{n(n-1)}{2}, n\right) & \xrightarrow{n \rightarrow \infty} & \left(\frac{1}{3}, 0\right).
 \end{array}$$

The truncated polytopes are the duals of the stacked polytopes, so they are simple. Similarly, the duals of cyclic polytopes are simple. Thus we find the four points  $(\frac{1}{10}, \frac{3}{10})$ ,  $(\frac{3}{10}, \frac{1}{10})$ ,  $(0, \frac{1}{3})$ , and  $(\frac{1}{3}, 0)$ , which span a quadrilateral subset of  $\text{proj}(\mathcal{F}_4)$ . This quadrilateral also represents the  $f$ -vectors of simple and of simplicial polytopes and “everything in between.” (Note that duality interchanges the coordinates  $\varphi_0$  and  $\varphi_3$ , and thus  $\text{proj}(\mathcal{F}_4)$  is symmetric with respect to the main diagonal.)

#### Five linear constraints we know:

$$\begin{array}{llll}
 \text{“Few Vertices”}: & f_0 \geq 5 & \iff & \varphi_0 \geq 0, \\
 \text{“Few Facets”}: & f_3 \geq 5 & \iff & \varphi_3 \geq 0, \\
 \text{“Simple”}: & f_1 \geq 2f_0 & \iff & 3\varphi_0 + \varphi_3 \leq 1, \\
 \text{“Simplicial”}: & f_2 \geq 2f_3 & \iff & \varphi_0 + 3\varphi_3 \leq 1, \\
 \text{“Lower bound”}: & 2f_1 + 2f_2 \geq 5f_0 + 5f_3 - 10 & \iff & \varphi_0 + \varphi_3 \leq \frac{2}{5}.
 \end{array}$$

The first four inequalities are quite trivial, and we have named them by the polytopes that satisfy them with equality, at least asymptotically. The translation into  $(\varphi_0, \varphi_3)$ -inequalities, using the Euler-Poincaré relation, poses no problem. There is no polytope with  $\varphi_0 = 0$ , but the condition is satisfied asymptotically by any family of 4-polytopes with far more vertices than facets. For example, the products of  $n$ -gons, with  $f(P_n \times P_n) = (n^2, 2n^2, n^2 + 2n, 2n)$ , yield  $(\varphi_0, \varphi_3) = (\frac{n^2-5}{3n^2+2n-20}, \frac{2n-5}{3n^2+2n-20}) \in \text{proj}(\mathcal{F}_4)$ , which in the limit  $n \rightarrow \infty$  yields  $(\frac{1}{3}, 0)$ .

The one non-trivial inequality in our table above is the last one, a “Lower Bound Theorem.” It may be derived quite easily [11] from the inequality  $f_{03} \geq 3f_0 + 3f_3 - 10$ , which was first established by Stanley [70] in terms of the so-called toric  $g$ -vector (it is the inequality “ $g_2^{\text{tor}}(P) \geq 0$ ”); a proof via rigidity theory was later given by Kalai [44].

Figure 4.3 summarizes our discussion up to this point: We are interested in  $\text{proj}(\mathcal{F}_4)$ , the closure of the set

$$\text{conv}\{(\varphi_0(P), \varphi_3(P)) : P \text{ is a 4-polytope, not a simplex}\} \subset \mathbb{R}^2.$$

This set is contained in the pentagon cut out by the five linear inequalities discussed above, and it contains the shaded trapezoid, which represents “everything between simple and simplicial polytopes.” Indeed, simple and simplicial polytopes satisfy the additional linear inequality  $\varphi_0 + \varphi_3 \geq \frac{1}{3}$ .

Thus we are left with the following “upper bound problem”:

**“Upper Bound Problem”.** Are there 4-polytopes with  $\varphi_0 + \varphi_3 \rightarrow 0$ ?

The inequality  $\varphi_0 + \varphi_3 \geq \frac{1}{3}$  is certainly not valid for all (possibly non-simple non-simplicial) 4-polytopes: Already for the hypersimplex we get  $(\varphi_0, \varphi_3) = (\frac{1}{8}, \frac{1}{8})$ .

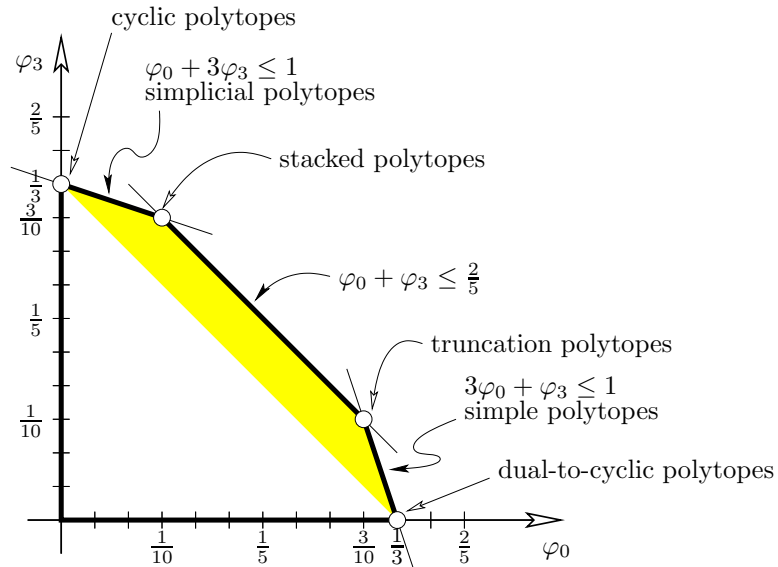


**Figure 4.3.** Projective representation of the  $f$ -vectors of 4-polytopes, in the  $(\varphi_0, \varphi_3)$ -plane. The convex set  $\text{proj}(\mathcal{F}_4)$  is contained in the bold pentagon; it contains the shaded trapezoid.

However, currently it is not clear how small  $\varphi_0 + \varphi_3$  can be for convex polytopes. Thus the Upper Bound Problem is the key remaining problem in the description of the  $f$ -cone for 4-polytopes.

- (!) If the answer is YES to the problem as posed above, then the five inequalities above constitute a complete linear description of  $\text{cone}(\mathcal{F}_4)$ .
- (!) If the answer is NO, then this is also exciting, since it means that the answers for cellular spheres and for convex polytopes are distinct! Indeed, cellular 3-spheres with arbitrarily small  $\varphi_0 + \varphi_3$  have been constructed by Eppstein, Kuperberg & Ziegler [26]; see our discussion in Section 4.3.

## 4.2. Fatness and the Upper Bound Problem

We prefer to rephrase the Upper Bound Problem in terms of a somewhat more graphic quantity, which we call “fatness.”

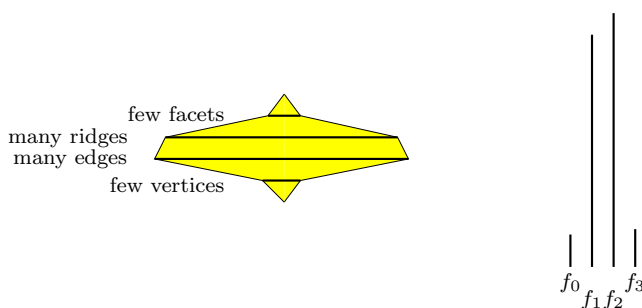


**Figure 4.4.** Fatness for a 4-polytope face lattice, and for an  $f$ -vector

**Definition 4.2** (Fatness). The *fatness* of a 4-polytope is the quotient

$$F(P) := \frac{1}{\varphi_0 + \varphi_3} = \frac{f_1 + f_2 - 20}{f_0 + f_3 - 10}.$$

The fatness of a 4-polytope is large if both  $\varphi_0$  and  $\varphi_3$  are small. This happens if the polytope has relatively few vertices and facets, but many edges and 2-faces. Thus, graphically, the face lattice and the  $f$ -vector are “fat in the middle,” whence the name (see Figure 4.4).

**“Upper Bound Problem”.** Can the fatness of a 4-polytope be arbitrarily large?

Here are a few explicit values to start with: For stacked and truncated 4-polytopes we have  $F(P) = \frac{5}{2}$  exactly. For cyclic polytopes we get  $F(C_4(n)) \rightarrow 3$  for  $n \rightarrow \infty$ , and the same for the duals — fatness is a self-dual quantity, that is, any 4-polytope and its dual have the same fatness. Moreover, it is easy to compute (or to derive from Figure 4.3) that all simple and simplicial polytopes satisfy  $\frac{5}{2} \leq F(P) < 3$ .

But how large can fatness be? The attempts to answer this question have led to a multitude of interesting examples and constructions, and to a fast succession of record holders for “the fattest examples found so far.” Many of them can be obtained by deep vertex truncation of simplicial polytopes, so they are 2-simple and 2-simplicial by Proposition 3.8:

- The hypersimplex, which is the dual of  $\text{DVT}(\Delta_4)$ , has fatness 4.
- Schäfli’s 24-cell [66],  $\text{DVT}(\text{cross polytope})$ , has fatness 4.526.
- Gévay’s 720-cell [36], the dual of  $\text{DVT}(120\text{-cell})$ , has 720 facets that are bipyramids over regular pentagons. It has fatness 5.020.
- Eppstein, Kuperberg & Ziegler [26] used hyperbolic geometry arguments to achieve a fatness of 5.048 by the “E-construction,” which is dual to deep vertex truncation.
- Paffenholz [55] has very recently shown that there are realizations for any sum of an  $n$ -gon and  $m$ -gon such that the deep vertex truncation  $\text{DVT}(P_m \times P_n)$  can be obtained. For  $m = n \rightarrow \infty$  this yields fatness approaching 6.

However, we’ll go a different route. In the next and final lecture we will present a construction that generalizes and extends the construction of “neighborly cubical” 4-polytopes of Joswig & Ziegler [43], to achieve fatness arbitrarily close to 9, the latest record (as far as I know at the time of writing). I would have been happy to have a “note added in proof” about this . . .

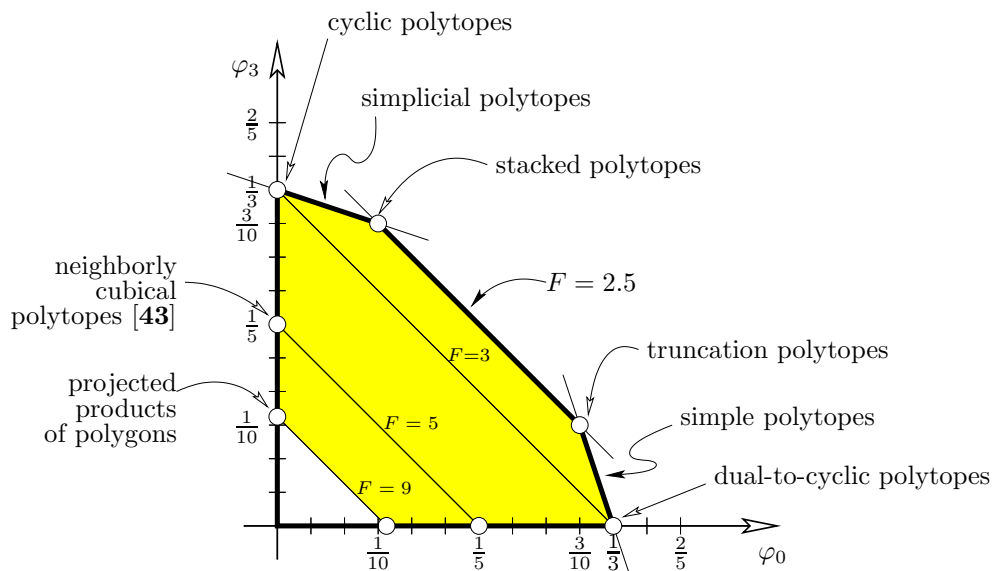


**Figure 4.5.** 4-polytopes in the  $(\varphi_0, \varphi_3)$ -plane. The shaded hexagon is spanned by the  $(\varphi_0, \varphi_3)$ -pairs of known 4-polytopes.

What do polytopes “of very high fatness” look like? You can verify (via Exercise 4.6) that they have two properties:

- (1) The facets have many vertices (on average).
- (2) The vertices are in many facets (on average).

Either of these properties are easy to satisfy — just look at the products  $P_n \times P_n$  for the first property, and at their duals, the free sums  $P_n \oplus P_n$ , for the second one. The key question is whether they can *simultaneously* be satisfied.

Finally, here is a problem on 3-dimensional polytopal tilings that is “essentially” equivalent to the fatness problem: Consider face-to-face tilings of  $\mathbb{R}^3$  (cf. [65]) that satisfy some regularity properties, e.g. one of the following (each implies the next):

- the tiling is triply periodic (that is, there are three linearly independent translational symmetries),
- there are only finitely many distinct congruence classes of tiles,
- in- and circumradius of the tiles are uniformly bounded.

For such tilings, we may define notions of “average” vertex degrees, face numbers, etc. The question is whether there is such a tiling where the tiles have lots of vertices on average, *and* the vertices are in many tiles on average. Again, either property is easy to achieve (look at tilings by Schlegel diagrams), but can they be *simultaneously* satisfied?

### 4.3. The Lower Bound Problem

The upper bound problem discussed here has a natural “lower bound” counterpart. It arises if we don’t restrict ourselves to the geometric model of convex polytopes, but consider the larger class of cellular spheres that are “regular” in the sense that their cells have no identifications on the boundary, and that satisfy the “intersection property” that any two faces should intersect in a single cell (which may be empty). These are the regular CW spheres [21] whose face poset is a lattice (where the meet operation corresponds to intersection of faces).

**“Lower Bound Problem”.** Does  $\varphi_0 + \varphi_3 \leq \frac{2}{5}$  hold for the cellular spheres that satisfy the intersection property?

This problem seems crucial in terms of the separation of the “geometric” model of convex polytopes from the “topological” model of cellular spheres/balls.

- (!) If the answer to the problem is NO, then this would establish such a separation, which would be quite remarkable.
- (!) If the answer is YES, then this would imply a complete characterization of the  $f$ -vector cone for cellular 3-spheres, by the five linear inequalities given above; indeed, Eppstein, Kuperberg & Ziegler [26] have constructed cellular spheres for which fatness is arbitrarily large, that is,  $\varphi_0 + \varphi_3$  is arbitrarily small.

We will not discuss this here further, but refer to [26] and [80].

### Exercises

- 4.1. Show that the two definitions of the  $f$ -vector cone given in Definition 4.1 are indeed equivalent.  
Hint: You need a separation lemma; see for example Matoušek [48, p. 6].
- 4.2. Show that the union of the line segments  $[f(\Delta_4), f(C_4(n))] \subset \mathbb{R}^4$  has the whole ray  $\{(5, 10 + t, 10 + 2t, 5 + t) : t \geq 0\}$  in its closure. Note that  $f_0 \geq 5$  is a valid linear inequality, which is tight at  $f(\Delta_4)$ , but for no other  $f$ -vector.  
Conclude that the cone with apex  $f(\Delta_4)$  spanned by the  $f$ -vectors of 4-polytopes is not closed.
- 4.3. Compute the fatness and the  $(\varphi_0, \varphi_3)$ -pair for the hypersimplex, the 24-cell, and for DVT(600-cell).
- 4.4. Compute the fatness of the 2s2s polytopes  $\text{DVT}(\text{Stack}(n, 4))$ , and show that it lies in the interval [4, 4.5).  
Show that for any simplicial 4-polytope  $P$ , the fatness of  $\text{DVT}(P)$  is smaller than 6.  
Where would the  $f$ -vectors of the polytopes  $\text{DVT}(P)$  lie in  $\text{proj}(\mathcal{F}_4)$ , as graphed in Figure 4.5?

- 4.5. If  $C_4^n$  is a cubical 4-polytope with the graph of an  $n$ -cube (see Exercise 3.2), compute the fatness and the pair  $(\varphi_0, \varphi_3)$ .
- 4.6. Define the *complexity* of a 4-polytope to be the quotient

$$C(P) := \frac{f_{03} - 20}{f_0 + f_3 - 10}.$$

- (a) Show that  $F(P) \leq 2C(P) - 2$ , with equality if and only if  $P$  is 2-simple and 2-simplicial.
- (b) Show that  $C(P) \leq 2F(P) - 2$ , with equality if and only if all facets of  $P$  are simple, or equivalently, if all vertex figures are simple.
- (c) Derive from this that fatness is high if and only if both the average number of vertices per facet,  $f_{03}/f_3$ , and the average number of facets per vertex,  $f_{03}/f_0$ , are large.

## LECTURE 5

### Projected Products of Polygons

In this lecture we present a construction of very recent vintage, “projected products of polytopes.” We will not have the ambition to work through all the technical details for this; these appear in [81], see also [63]; rather, our main objective is here to identify the structural features of the construction which lead to fat polytopes, and to outline (possibly “for further use”) some interesting components that go into the construction. In the following version of the main result, some concepts that will be explained below are highlighted by quotation marks.

**Theorem 5.1** (Ziegler [81]). *For each  $r \geq 2$ , and even  $n \geq 4$ , there is a realization  $P_n^r \subset \mathbb{R}^{2r}$  of a product of polygons  $(P_n)^r$  (a “deformed product of polygons”) such that the vertices and edges and all the “ $n$ -gon 2-faces” of  $P_n^r$  “survive” the projection  $\pi : \mathbb{R}^{2r} \rightarrow \mathbb{R}^4$  to the last 4 coordinates.*

A number of nice tricks go into the construction that proves the theorem — see below. Before we look into these we want to derive the enumerative consequences: The  $f$ -vector of  $\pi(P_n^r)$  can be derived purely from the information given in the theorem, not using details about the combinatorics of the resulting polytopes (which were worked out only recently [62] [63]).

#### 5.1. Products and deformed products

We have discussed the construction and main properties of products of polytopes already in Example 2.7. A key observation is that the non-empty faces of a product are the products of non-empty faces of the “factors.” Now we specialize to the case of products of (several) polygons: We consider products of  $r$   $n$ -gons — and later we will be looking at polytopes that just have the combinatorics of such polytopes.

If  $P_n$  is an  $n$ -gon, then  $(P_n)^r$  is a simple polytope of dimension  $2r$ . It has

- $f_0 = n^r$  vertices (of the form “vertex  $\times$  vertex  $\times$  . . . . .  $\times$  vertex”), and
- $f_1 = rn^r$  edges (of the form “vertex  $\times$  . . .  $\times$  edge  $\times$  . . .  $\times$  vertex”).

The products of polygons have two different types of 2-faces, “quadrilaterals” and “polygons,” that we need to distinguish:

- $\binom{r}{2}n^r$  quadrilateral 2-faces (which arise as products of two edges, and vertices from the other factors), and
- $rn^{r-1}$  polygon 2-faces (arising as a product of one  $n$ -gon factor with vertices from the other factors).

Thus we get  $f_2 = \binom{r}{2}n^r + rn^{r-1}$ .

Finally, let's note that  $(P_n)^r$  has  $nr$  facets, which arise as a product of one edge (from one of the factors) with  $n$ -gons as the other factors.

The “deformed products” of polygons  $P_n^r$  considered below are combinatorially equivalent to the “orthogonal products”  $(P_n)^r$ . Thus, the  $f$ -vector count given here is valid for deformed products as well.

## 5.2. Computing the $f$ -vector

It is remarkable that for the proof of the following corollary to Theorem 5.1 we don't need detailed combinatorial information about  $\pi(P_n^r)$ ; it is sufficient to know that it is a generic projection of a deformed product  $P_n^r$ , and that all the polygon 2-faces survive the projection. The facets of  $\pi(P_n^r)$  are 3-faces of  $P_n^r$  that “have survived the projection,” that is, they are combinatorial cubes and prisms over  $n$ -gons.

**Corollary 5.2.**  $\pi(P_n^r) \subset \mathbb{R}^4$  is a 4-polytope with  $f$ -vector

$$\begin{aligned} & (n^r, rn^r, \frac{5}{4}rn^r - \frac{3}{4}n^r + rn^{r-1}, \frac{1}{4}rn^r - \frac{1}{2}n^r + rn^{r-1}) \\ &= (0 + \frac{4}{r}, 4, 5 - \frac{3}{r} + \frac{4}{n}, 1 - \frac{2}{r} + \frac{4}{n}) \cdot \frac{1}{4}rn^r. \end{aligned}$$

*In particular, for  $n, r \rightarrow \infty$  the fatness of the projected products of polygons  $\pi(P_n^r)$  gets arbitrarily close to 9.*

**Proof.** From the combinatorial information above we see that each vertex, and each edge, of a product of polygons  $(P_n)^r$  is contained in a polygon 2-face: So if all the polygon 2-faces survive the projection, then in particular all vertices and edges do. Thus, for  $(f_0, f_1, f_2, f_3) := f(\pi(P_n^r))$  we get  $f_0 = n^r$ , and  $f_1 = rn^r$ .

Furthermore, we know that  $\pi(P_n^r)$  has  $p := rn^{r-1}$  polygon 2-faces (and a yet unknown number of quadrilaterals). Moreover, the facets of  $\pi(P_n^r)$  are prisms over polygons, and cubes. Each prism has two polygon faces (and  $n$  quadrilateral faces), while each cube has 6 quadrilateral 2-faces, but no polygon faces. So, each polygon (ridge!) lies in two prism facets, and each prism facet contains two polygons: Double counting yields that there are exactly  $p = rn^{r-1}$  prism facets.

Denote by  $c$  the number of cube facets. Then we have

- $f_3 = c + p$  (all facets are cubes or prisms),
- $2f_2 = 6c + (n + 2)p$  (double counting the facet-ridge incidences), and
- $f_2 - f_3 = (r - 1)n^r$  (Euler's equation).

These three linear equations can now be solved for the three unknowns,  $f_2$ ,  $f_3$ , and  $c$ .  $\square$

## 5.3. Deformed products

A number of different polytope constructions have been studied in attempts to produce interesting polytopes. For example, *any* polytope may be obtained by projection of a simplex; on the other hand, any projection of an orthogonal cube is a zonotope, which is a polytope of very special structure (see [79, Lect. 7]). The projections of orthogonal products of centrally symmetric polygons are still zonotopes, and the projections of orthogonal products of arbitrary polygons are only a bit more general. However, it has been noted since the seventies (in the context of linear programming, trying to construct “bad examples” for the simplex





with a block-diagonal matrix of size  $rn \times 2r$ , which describes the orthogonal product of polygons  $(P_n)^r \subset \mathbb{R}^n$ .

The combinatorics of the product of polygons is reflected in the facet-vertex incidences, as follows: Each inequality defines a facet; each of the  $n^r$  vertices is the unique solution of a linear system of equations that is obtained by requiring that from each block, two cyclically adjacent inequalities are tight.

*Deformed product of polygons:* Our Ansatz is as follows:

$$(5.1) \quad \left( \begin{array}{cccc} V^\varepsilon & & & \\ W & V^\varepsilon & & \\ U & W & V^\varepsilon & \\ & U & W & \ddots \\ & & & \ddots \\ & & & & V^\varepsilon \\ & & & & U & W & V^\varepsilon \\ & & & & & U & W & V^\varepsilon \end{array} \right) x \leq \begin{pmatrix} b_1 \\ b_2 \\ b_3 \\ \vdots \\ b_{r-1} \\ b_r \end{pmatrix}.$$

If the diagonal  $V^\varepsilon$ -blocks  $V^\varepsilon \in \mathbb{R}^{n \times 2}$  satisfy the conditions above, then the blocks  $U, W \in \mathbb{R}^{n \times 2}$  below the diagonal blocks can be arbitrary — the right-hand sides can be adjusted in such a way that we get a *deformed product*, which is combinatorially equivalent to a product  $(P_n)^r$ .

For this, we only have to verify that we get the correct combinatorics: If for each of the  $r$  blocks we choose two cyclically adjacent inequalities and require them to be tight, then this should yield a linear system of equations with a unique solution, for which all other inequalities are satisfied, but not tight. It is now easy to prove (by induction on  $r$ ) that our system satisfies this — if we just choose the right-hand sides suitably; in particular,  $b_i := M^{i-1}b \in \mathbb{R}^n$  works, for large enough  $M$ , if  $V^\varepsilon x \leq b$  (as above) defines an  $n$ -gon.

**Example 5.3.** To illustrate this in a simple case, let's consider deformed products in the low-dimensional case of  $I \times I$ , a square, where  $I$  denotes an interval (a 1-dimensional polytope) such as  $I = [0, 1]$ .

In this case  $I$  can be written as

$$I = \left\{ x \in \mathbb{R} : \begin{pmatrix} -1 \\ 1 \end{pmatrix} x \leq \begin{pmatrix} 0 \\ 1 \end{pmatrix} \right\}.$$

Consequently, the product  $I \times I$  may be represented by

$$I \times I = \left\{ x \in \mathbb{R}^2 : \begin{pmatrix} -1 & 0 \\ 1 & 0 \\ 0 & -1 \\ 0 & 1 \end{pmatrix} x \leq \begin{pmatrix} 0 \\ 1 \\ 0 \\ 1 \end{pmatrix} \right\}.$$

Now changing the matrix into

$$\begin{pmatrix} -1 & 0 \\ 1 & 0 \\ a & -1 \\ b & 1 \end{pmatrix} x \leq \begin{pmatrix} 0 \\ 1 \\ 0 \\ 1 \end{pmatrix}$$

leaves the first two inequalities (and thus the first  $I$  factor) intact, but it changes the slopes of the other two inequalities — and if you are unlucky (that is, for  $a + b > 1$ ) the resulting polytope will not be equivalent to  $I \times I$  any more. This situation is depicted in the middle part of Figure 5.2. However, it can be remedied by increasing right-hand sides: For any given  $a$  and  $b$ , a suitably large  $M$ , namely  $M > a + b$ , in

$$\begin{pmatrix} -1 & 0 \\ 1 & 0 \\ a & -1 \\ b & 1 \end{pmatrix} x \leq \begin{pmatrix} 0 \\ 1 \\ 0 \\ M \end{pmatrix}$$

will result in a product again (as in the right part of Figure 5.2).

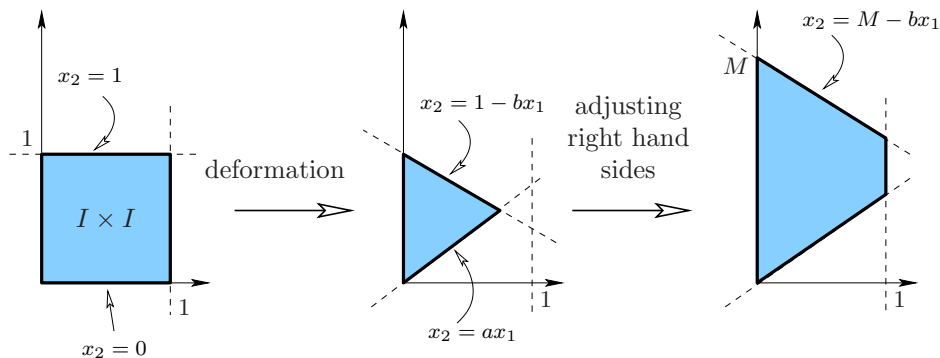


**Figure 5.2.** Construction of a deformation of  $I \times I$

### 5.4. Surviving a generic projection

We are looking at *generic projections* of *simple polytopes* — that is, the direction of projection is in general position with respect to all the edges of the polytope to be projected, and thus a small perturbation of the inequalities of the polytope, and of the direction of projection, will not change the combinatorics of the projected polytope.

It should thus seem plausible that in this setting the following holds (compare Figure 5.3) for a polytope projection  $\pi : P \rightarrow \pi(P)$ :

- The normal vectors to a face  $G \subset P$  are the positive linear combinations of the (defining) normal vectors  $n_F$  to all the facets  $F \supset G$  that contain  $G$ .
- The proper faces of  $\pi(P)$  are isomorphic copies of the faces of  $P$  that *survive* the projection.
- A face  $G \subset P$  survives the projection exactly if it has a normal vector that is orthogonal to the direction of projection.

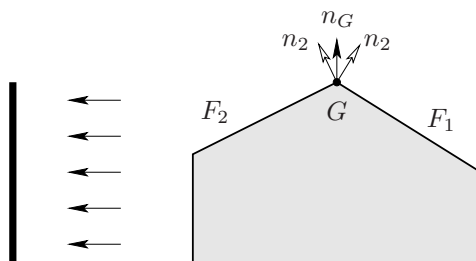


**Figure 5.3.** A vertex  $G$  surviving a projection, a normal vector  $n_G$  orthogonal to the projection, and the normal vectors  $n_1$  and  $n_2$  of facets  $F_1$  and  $F_2$  it can be combined from

For Theorem 5.1 we have to specify a deformed product realization for  $(P_n)^r$  of the type given in Ansatz (5.1), such that all  $n$ -gon 2-faces are strictly preserved by the projection. That is,

- if we choose two cyclically adjacent rows from each block except for one, and
- truncate these rows to the first  $2r - 4$  coordinates,

then the resulting  $2r - 2$  vectors must be positively dependent and span.

### 5.5. Construction

Now we want to specify the lower-triangular block matrix in our Ansatz (5.1) so that it satisfies the following two main properties:

- (1) the diagonal blocks have “rows in cyclic order,” and
- (2) any “choice of two cyclically adjacent rows” from all but one of the blocks, truncated to the first  $2r - 4$  components, yields a positively-spanning set of vectors.

Five observations (you may call them “tricks”) help us to achieve this:

- (i) Condition (2) is stable under perturbation. So, we first construct a matrix that satisfies (2), then perturb it in order to achieve (1).

(The diagonal blocks of the matrix that we construct to satisfy (2) are denoted  $V$ ; after perturbation, they will be  $V^\varepsilon$ .)

- (ii) The submatrices  $V$ ,  $W$ , and  $U$  of size  $n \times 2$  are constructed to have alternating rows: So if you choose two cyclically adjacent rows from a block, you know what you get!

Specifically, we will let matrix  $V$  have rows that alternate between  $(1, 0)$  and  $(0, 0)$ , matrix  $W$  gets rows  $(0, 1)$  and  $(a, b)$ , and matrix  $U$  gets rows  $(c, d)$  and  $(e, f)$ , with the six parameters  $a, b, c, d, e, f$  to be determined.

- (iii) To make sure that you get the positive linear dependence for (2), we specify a positive coefficient sequence and compute the matrix entries to satisfy them.
- (iv) Rather than admitting that from one of the blocks no row is chosen, we will prescribe coefficient sequences that could have zeroes on any one of the blocks, which yields linear dependencies for which the vectors from one block are “not used.”

Specifically, we take coefficient sequences of the form  $\alpha_k := (2^{k-t} - 1)^2$  and  $\beta_k := (2^{k-t} - 1)(2^{k-t} - \frac{3}{2})$  for the odd resp. even-index rows. These coefficients are clearly positive for integral  $k$ , except they vanish at  $k = t$ .

Moreover, they are linear combinations of the three exponential functions  $2^{k-t}$ ,  $4^{k-t}$ , and 1. If we write out the condition that “the rows chosen should be dependent, with coefficients  $\alpha_k$  (for the even-index row chosen from the  $k$ -th block) and  $\beta_k$  (for the odd-index row chosen from the  $k$ -th block), then this leads to a system of six linear equations, in six unknowns  $a, b, c, d, e, f$  — solve it!

- (v) The properties “alternating rows” and “rows in cyclic order” are, of course, incompatible — but a matrix with rows in cyclic order can be obtained as a perturbation  $V^\varepsilon$  of the matrix  $V$  that has rows  $(1, 0)$  and  $(0, 0)$  in alternation. Figure 5.4 suggests a way to do this.

This completes our sketch of “how to do it” — it should be sufficient to let you construct the polytopes  $P_n^r$  and thus prove Theorem 5.1 (but [81] provides these details, too.)

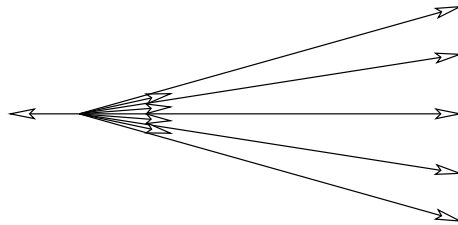


**Figure 5.4.** A configuration of 10 vectors, which positively span the plane, and which (in cyclic order) alternate between vectors close to  $(1, 0)$ , and close to  $(0, 0)$

If you think about this construction, can you perhaps manage to simplify some of the details, or even to improve the construction? After all, on the way to the characterization of the  $f$ -vector cone for 4-polytopes, this construction of polytopes of fatness up to 9 should be taken just as an intermediate step. Can you get further? There is a long way to go from 9 to infinity . . .

**Exercises**

- 5.1. Show that every polytope arises as a projection of a simplex.
- 5.2. Show that if  $\pi : \mathbb{R}^n \rightarrow \mathbb{R}^d$ ,  $P \rightarrow \pi(P)$  is a polytope projection, for an  $n$ -polytope  $P$ , and  $n > d$ , then the strictly preserved faces have dimension at most  $d - 1$ . In particular, no facet of  $P$  is strictly preserved by the projection.
- 5.3. Give examples of polytope projections where no faces are strictly preserved.
- 5.4. Realize the prism over an  $n$ -gon ( $n \geq 3$ ) in such a way that the projection  $\mathbb{R}^3 \rightarrow \mathbb{R}^2$  strictly preserves all  $2n$  vertices.
- 5.5. Show that the product  $\Delta_2 \times \Delta_2$  of two triangles cannot be realized in such a way that all 9 vertices are strictly preserved in a projection to  $\mathbb{R}^2$ .
- 5.6. How large do we have to choose  $r$  and  $n$  in order to obtain 4-polytopes of fatness  $F(\pi(P_n^r)) > 8$ ?
- 5.7. Any projection of a (non-deformed) product of centrally symmetric polygons is a *zonotope*. For these, one knows that  $f_1 < 3f_0$  (for such inequalities, for the dual polytope, see [16, pp. 198/199]). Deduce from this information that the fatness is smaller than 5.

## APPENDIX: A SHORT INTRODUCTION TO POLYMAKE

by Thilo Schröder and Nikolaus Witte

The software project `polymake` [31] has been developed since 1997 in the Discrete Geometry group at TU Berlin by Ewgenij Gawrilow and Michael Joswig, with contributions by several others. It was initially designed to work with convex polytopes. Due to its open design the `polymake` framework can also be used on other types of objects; the current release includes a second application, `topaz`, which treats simplicial complexes.

`polymake` is designed to run on any Linux or Unix system, including Mac OS X. It runs in a shell using command line input. This introduction is for `polymake` versions 2.0 and 2.1. `polymake` is free software and you can redistribute it and/or modify it under the terms of the GNU General Public License as published by the Free Software Foundation.

This introduction aims at getting you to work on the computer rather than explaining the details about the machinery of `polymake`. Therefore, there will be only a short description of the software design, in Section A.2. For further reading we refer to Gawrilow & Joswig [32] [33]. On the `polymake` website

<http://www.math.tu-berlin.de/polymake>

you will find extensive *online documentation* as well as an introductory *tutorial*.

### A.1. Getting Started

For `polymake`, every polytope is treated as an *object* (the file storing the data) with certain *properties* such as its  $f$ -vector, its Hasse diagram, etc. The  $\mathcal{V}$ - and  $\mathcal{H}$ -representation are also regarded as properties, and any one of them may be used to define the polytope in the first place. If you are only interested in the combinatorial structure you may also input the vertex-facet incidences. For more details concerning the `polymake` file format see Section A.1.3. Once a polytope is defined in terms of some property, you may ask `polymake` to compute further properties.

`polymake` also provides standard constructions for polytopes. You can either construct polytopes from scratch (e.g. the  $d$ -cube) or by applying constructions to

an existing polytope (e.g. the pyramid). In both cases `polymake` will produce a new file defining the new polytope.

This section explains the command line syntax of `polymake` for constructing, analyzing and visualizing polytopes. The `polymake` file format is briefly described at the end of this section.

### A.1.1. Constructions of Polytopes

If you want to use one of `polymake`'s constructions, you have to call a *client program* to create the polytope. The clients have appropriate names, e.g. the client producing the  $d$ -cube is called `cube`. All clients are documented at [31]. If in doubt about the exact syntax of a client program just type the client's name, press return and you will get a *usage* message.

#### Clients producing polytopes from scratch

The basic syntax to create a polytope from scratch is the command line

```
<client> <file> [ <options> ]
```

For example, to produce a 4-cube type

```
cube c4.poly 4
```

Some other clients which produce polytopes you might have heard of are `simplex`, `cyclic`, `cross`, `rand_sphere`, `associahedron`, and `permutahedron`.

#### Clients producing polytopes from others

To construct a polytope from existing one(s), use

```
<client> <out_file> <in_file> [ <options> ]
```

For example, to produce the pyramid over our 4-cube `c4.poly` type

```
pyramid c4.pyr.poly c4.poly
```

Some other constructions to get interesting polytopes are obtained via the clients `bipyramid`, `prism`, `minkowski_sum`, `vertex_figure`, `center`, `truncation`, and `polarize`.

### A.1.2. Computing Properties and Visualizing

To compute a property of a polytope, just ask `polymake` using the following syntax

```
polymake <file> <PROPERTY_1> <PROPERTY_2> ...
```

The properties are written in capital letters. To compute the numbers of facets and vertices of the pyramid over the 4-cube constructed above, type

```
polymake c4.pyr.poly N_FACETS N_VERTICES
```

Some other useful properties are

```
GRAPH, DUAL_GRAPH, HASSE_DIAGRAM, CENTERED, VERTICES_IN_FACETS, F_VECTOR,
H_VECTOR, SIMPLE, SIMPLICIAL, CUBICAL, SIMPLICIALITY, and SIMPLICITY.
```

The visualizations use the same syntax. For example, to take a look at the graph of a polytope, just use

```
polymake my.poly VISUAL_GRAPH
```

Here are some more visualizations

```
VISUAL, SCHLEGEL, VISUAL_FACE_LATTICE, and VISUAL_DUAL_GRAPH.
```



### A.1.3. File Format

Let's have a brief look at the `polymake` file format. If you have a look at the file `c4.pyr.poly`, you will find a paragraph for each property. The paragraphs are headed by the property's name in capital letters, followed by the data. The `VERTICES` and `POINTS` are represented in *homogeneous* coordinates, where the first coordinate is used for homogenization. The inequality  $a_0 + a_1x_1 + \dots + a_dx_d \geq 0$  is encoded as the vector  $(a_0 \ a_1 \ \dots \ a_d)$ .

To define a polytope with your own  $\mathcal{V}$ - or  $\mathcal{H}$ -description you should create a file that contains a `POINTS` or `INEQUALITIES` section.

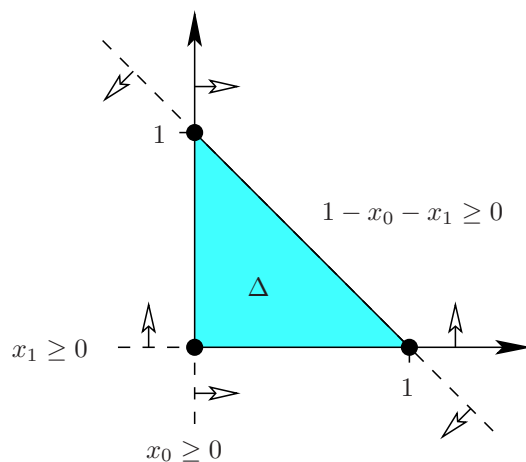


**Figure A.1.** The triangle  $\Delta$  and its  $\mathcal{V}$ - and  $\mathcal{H}$ -description.

**Example.** If you want to construct the triangle  $\Delta$  (cf. Figure A.1) that is given as

$$\Delta := \text{conv}\{(0, 0), (0, 1), (1, 0)\}$$

your input file should look as follows (homogeneous coordinates):

```
POINTS
1 0 0
1 0 1
1 1 0
```

If you prefer to enter the same example by the inequality description

$$\Delta := \{x \in \mathbb{R}^2 : 1 - x_0 - x_1 \geq 0, x_0 \geq 0, x_1 \geq 0\},$$

this should be your `polymake` file:

```
INEQUALITIES
1 -1 -1
0 1 0
0 0 1
```

The difference between `POINTS` and `VERTICES` is that the former may contain redundancies. So you should enter `POINTS`, but ask for `VERTICES`. Similarly, one should enter `INEQUALITIES` and ask for `FACETS`.

## A.2. The polymake System

The world seen through the eyes of the `polymake` system consists of *objects* with *properties*. For a given object you may ask for one of its properties and `polymake` will compute it. Yet `polymake` acts only as a framework for the computation, knowing little about the math involved. The actual computations are delegated to client programs. The open design, keeping the system and the math independent, allows for the use of external software as clients. It also makes `polymake` extremely flexible with respect to the kind of objects you want to examine. For example the applications `polytope` and `topaz` examine different classes of geometric objects.

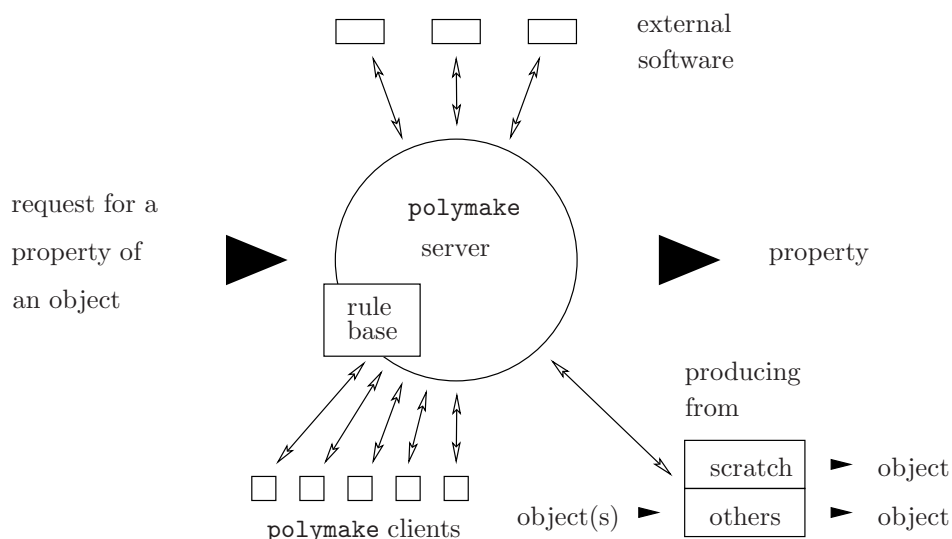


Figure A.2. Main components of the `polymake` system.

The `polymake` system consists of the following three components as illustrated in Figure A.2:

- The `polymake server` together with the *rule base*.
- `polymake client` programs computing properties and new objects.
- External software, such as the `cdd` [28] convex hull algorithm or the `JavaView` [58] visualization package.

The rule base is a collection of rules, each rule containing a set of input and output properties and an algorithm (that is a client or external software) which computes the output properties *directly* from the input properties. If you request a property of an object, the server has to determine how to compute the requested property from the ones which are already known. There might not be an algorithm computing the requested property directly, so other properties might have to be computed first. Therefore, the server has to compose a sequence of rules (from the rule base) to be executed in order to compute the requested property.

### Examples and Exercises

- A.1. Construct the  $d$ -simplex and the  $d$ -cube for  $d = 3, 4, 5$ . Visualize the face lattice of the polytope and its Schlegel diagram (see Section 3.1).
- A.2. Construct the cyclic polytopes  $C_3(7)$  and  $C_4(8)$ . Visualize and check Gale's evenness criterion (see Example 2.6). Alternatively, try constructing  $C_4(8)$  using the client `cyclic_caratheodory`. What is the difference?
- A.3. Produce the dual polytopes of the polytopes above. Watch out, they have to be **CENTERED**. (Check the documentation [31] for the property **CENTERED**)
- A.4. Construct an octahedron using as many different ways as possible.
- A.5. Build the bipyramid over a square, truncate both apexes and polarize. What does the resulting polytope look like?
- A.6. Construct the product of a 5-gon and a 7-gon and visualize it.
- A.7. Construct a 4-polytope with the `pcmi` logo as its Schlegel diagram.



- A.8. Use the client `rand_sphere` to create a random polytope by uniformly distributing 1000 points on the unit 2-sphere, visualize it and compare it to Figure 1.4. Take a look at its `VERTEX_DEGREES` and cut off a vertex of maximal degree.
- A.9. Take a 3-polytope and truncate all its vertices. Is the resulting polytope always simple?
- A.10. Truncate the vertices of the 4-dimensional cross polytope, and let `polymake` compute the  $f$ -vector, and whether the resulting polytope is simple. Can you justify the results theoretically?
- A.11. For a given planar 3-connected graph  $G$  containing a triangular face, produce a 3-polytope with  $G$  as its graph (see Section 1.2). Use the client `tutte_lifting`.
- A.12. Visualize the Schlegel diagrams of the `dwarfed_cube` that you get by using different projection facets.
- A.13. Visualize the effect of standard constructions (such as truncation, stellar subdivision) on the Schlegel diagrams of 4-polytopes.



## BIBLIOGRAPHY

1. R. K. AHUJA, T. L. MAGNANTI, AND J. B. ORLIN, *Network flows*, Prentice Hall Inc., Englewood Cliffs, NJ, 1993
2. M. AIGNER AND G. M. ZIEGLER, *Proofs from THE BOOK*, Springer-Verlag, Heidelberg Berlin, third ed., 2004
3. N. AMENTA AND G. M. ZIEGLER, *Shadows and slices of polytopes*, in Proceedings of the 12th Annual ACM Symposium on Computational Geometry, May 1996, pp. 10–19
4. ———, *Deformed products and maximal shadows*, in Advances in Discrete and Computational Geometry (South Hadley, MA, 1996), B. Chazelle, J. E. Goodman, and R. Pollack, eds., vol. 223 of Contemporary Mathematics, Providence RI, 1998, Amer. Math. Soc., pp. 57–90
5. E. M. ANDREEV, *On convex polyhedra in Lobačevskiĭ spaces*, Math. of the USSR — Sbornik, 10 (1970), pp. 445–478. Translation from Math. Sbornik (N.S.) 81 (123) (1970), pp. 445–478
6. M. L. BALINSKI, *On the graph structure of convex polyhedra in  $n$ -space*, Pacific J. Math., 11 (1961), pp. 431–434
7. D. W. BARNETTE, *Projections of 3-polytopes*, Israel J. Math., 8 (1970), pp. 304–308
8. ———, *The projection of the  $f$ -vectors of 4-polytopes onto the  $(E, S)$ -plane*, Discrete Math., 10 (1974), pp. 201–216
9. D. W. BARNETTE AND B. GRÜNBAUM, *Preassigning the shape of a face*, Pacific J. Math., 32 (1970), pp. 299–302
10. D. W. BARNETTE AND J. R. REAY, *Projections of  $f$ -vectors of four-polytopes*, J. Combinatorial Theory, Ser. A, 15 (1973), pp. 200–209
11. M. M. BAYER, *The extended  $f$ -vectors of 4-polytopes*, J. Combinatorial Theory, Ser. A, 44 (1987), pp. 141–151
12. L. J. BILLERA AND C. W. LEE, *A proof of the sufficiency of McMullen's conditions for  $f$ -vectors of simplicial polytopes*, J. Combinatorial Theory, Ser. A, 31 (1981), pp. 237–255
13. A. BJÖRNER, *The unimodality conjecture for convex polytopes*, Bulletin Amer. Math. Soc., 4 (1981), pp. 187–188
14. ———, *Face numbers of complexes and polytopes*, in Proceedings of the International Congress of Mathematicians (Berkeley CA, 1986), 1986, pp. 1408–1418

15. ———, *Partial unimodality for  $f$ -vectors of simplicial polytopes and spheres*, in Jerusalem Combinatorics '93, H. Barcelo and G. Kalai, eds., vol. 178 of Contemporary Math., Providence RI, 1994, Amer. Math. Soc., pp. 45–54
16. A. BJÖRNER, M. LAS VERGNAS, B. STURMFELS, N. WHITE, AND G. M. ZIEGLER, *Oriented Matroids*, vol. 46 of Encyclopedia of Mathematics, Cambridge University Press, Cambridge, second (paperback) ed., 1999
17. A. I. BOBENKO AND B. A. SPRINGBORN, *Variational principles for circle patterns, and Koebe's theorem*, Transactions Amer. Math. Soc., 356 (2004), pp. 659–689
18. T. BRADEN, *A glued hypersimplex*. Personal communication, 1997
19. F. BRENTI, *Log-concave and unimodal sequences in algebra, combinatorics, and geometry: an update*, in Jerusalem Combinatorics '93, vol. 178 of Contemp. Math., Amer. Math. Soc., Providence, RI, 1994, pp. 71–89
20. Y. COLIN DE VERDIÈRE, *Un principe variationnel pour les empilements de cercles*, Inventiones Math., 104 (1991), pp. 655–669
21. G. E. COOKE AND R. L. FINNEY, *Homology of Cell Complexes*, Princeton University Press, Princeton NJ, 1967
22. H. S. M. COXETER, *Regular Polytopes*, Macmillan, New York, second ed., 1963. Corrected reprint, Dover, New York 1973
23. J. DE LOERA, B. STURMFELS, AND R. R. THOMAS, *Gröbner bases and triangulations of the second hypersimplex*, Combinatorica, 15 (1995), pp. 409–424
24. J. ECKHOFF, *Combinatorial properties of  $f$ -vectors of convex polytopes*. Unpublished manuscript, Dortmund 1985
25. D. EPPSTEIN, *Nineteen proofs of Euler's formula:  $V - E + F = 2$* . The Geometry Junkyard, <http://www.ics.uci.edu/~eppstein/junkyard/euler/>, October 2005
26. D. EPPSTEIN, G. KUPERBERG, AND G. M. ZIEGLER, *Fat 4-polytopes and fat-ter 3-spheres*, in Discrete Geometry: In honor of W. Kuperberg's 60th birthday, A. Bezdek, ed., vol. 253 of Pure and Applied Mathematics, Marcel Dekker Inc., New York, 2003, pp. 239–265, <http://www.arXiv.org/math.CO/0204007>
27. P. J. FEDERICO, *Descartes on Polyhedra*. A study of the *De solidorum elementis*, vol. 4 of Sources in the History of Mathematics and Physical Sciences, Springer-Verlag, New York, 1982
28. K. FUKUDA, *CDD and CDD+ — implementations of the double description method*, [http://www.ifor.math.ethz.ch/~fukuda/cdd\\_home/](http://www.ifor.math.ethz.ch/~fukuda/cdd_home/)
29. A. M. GABRIÉLOV, I. M. GEL'FAND, AND M. V. LOSIK, *Combinatorial computation of characteristic classes*, Functional Analysis Appl., 9 (1975), pp. 103–115
30. D. GALE, *Neighborly and cyclic polytopes*, in Convexity, V. Klee, ed., vol. VII of Proc. Symposia in Pure Mathematics, Providence RI, 1963, Amer. Math. Soc., pp. 225–232
31. E. GAWRILOW AND M. JOSWIG, *Polymake: A software package for analyzing convex polytopes*, <http://www.math.tu-berlin.de/diskregeom/polymake/>
32. ———, *Polymake: A framework for analyzing convex polytopes*, in Polytopes — Combinatorics and Computation, G. Kalai and G. M. Ziegler, eds., vol. 29 of DMV Seminar, Birkhäuser-Verlag, Basel, 2000, pp. 43–73

33. ———, *Geometric reasoning with POLYMAKE*, Preprint, July 2005, 13 pages, <http://www.arxiv.org/math/0507273>
34. I. M. GELFAND, M. M. KAPRANOV, AND A. V. ZELEVINSKY, *Discriminants, Resultants, and Multidimensional Determinants*, Birkhäuser, Boston, 1994
35. I. M. GELFAND AND R. D. MACPHERSON, *Geometry in Grassmannians and a generalization of the dilogarithm*, *Advances in Math.*, 44 (1982), pp. 279–312
36. G. GÉVAY, *Kepler hypersolids*, in *Intuitive geometry* (Szeged, 1991), vol. 63 of *Colloq. Math. Soc. János Bolyai*, Amsterdam, 1994, North-Holland, pp. 119–129
37. D. GOLDFARB, *On the complexity of the simplex algorithm*, in *Advances in optimization and numerical analysis. Proc. 6th Workshop on Optimization and Numerical Analysis*, Oaxaca, Mexico, January 1992, Dordrecht, 1994, Kluwer, pp. 25–38. Based on: *Worst case complexity of the shadow vertex simplex algorithm*, preprint, Columbia University 1983, 11 pages
38. M. GRÖTSCHEL, *Cardinality homogeneous set systems, cycles in matroids, and associated polytopes*, in *The Sharpest Cut: The Impact of Manfred Padberg and His Work*, M. Grötschel, ed., MPS-SIAM, 2004, pp. 99–120
39. B. GRÜNBAUM, *Convex Polytopes*, vol. 221 of *Graduate Texts in Math.*, Springer-Verlag, New York, 2003. Second edition prepared by V. Kaibel, V. Klee and G. M. Ziegler (original edition: Interscience, London 1967)
40. M. HENK, J. RICHTER-GEBERT, AND G. M. ZIEGLER, *Basic properties of convex polytopes*, in *Handbook of Discrete and Computational Geometry*, J. E. Goodman and J. O'Rourke, eds., Chapman & Hall/CRC Press, Boca Raton, second ed., 2004, ch. 16, pp. 355–382
41. D. HILBERT AND S. COHN-VOSSEN, *Anschauliche Geometrie*, Springer-Verlag, Berlin Heidelberg, 1932. Second edition 1996. English translation: *Geometry and the Imagination*, Chelsea Publ., 1952
42. A. HÖPPNER AND G. M. ZIEGLER, *A census of flag-vectors of 4-polytopes*, in *Polytopes — Combinatorics and Computation*, G. Kalai and G. M. Ziegler, eds., vol. 29 of *DMV Seminars*, Birkhäuser-Verlag, Basel, 2000, pp. 105–110
43. M. JOSWIG AND G. M. ZIEGLER, *Neighborly cubical polytopes*, *Discrete & Computational Geometry* (Grünbaum Festschrift: G. Kalai, V. Klee, eds.), (2-3)24 (2000), pp. 325–344, <http://www.arXiv.org/math.CO/9812033>
44. G. KALAI, *Rigidity and the lower bound theorem, I*, *Inventiones Math.*, 88 (1987), pp. 125–151
45. V. KLEE AND G. J. MINTY, *How good is the simplex algorithm?*, in *Inequalities, III*, O. Shisha, ed., Academic Press, New York, 1972, pp. 159–175
46. P. KOEBE, *Kontaktprobleme der konformen Abbildung*, *Berichte Verh. Sächs. Akademie der Wissenschaften Leipzig, Math.-Phys. Klasse*, 88 (1936), pp. 141–164
47. C. W. LEE, *Counting the faces of simplicial polytopes*, Ph.D. thesis, Cornell University, 1981, 171 pages
48. J. MATOUŠEK, *Lectures on Discrete Geometry*, vol. 212 of *Graduate Texts in Math.*, Springer-Verlag, New York, 2002
49. J. C. MAXWELL, *On reciprocal figures and diagrams of forces*, *Philosophical Magazine*, Ser. 4, 27 (1864), pp. 250–261
50. B. MOHAR, *A polynomial time circle packing algorithm*, *Discrete Math.*, 117 (1993), pp. 257–263

51. K. G. MURTY, *Computational complexity of parametric linear programming*, Math. Programming, 19 (1980), pp. 213–219
52. S. ONN AND B. STURMFELS, *A quantitative Steinitz' theorem*, Beiträge zur Algebra und Geometrie/Contributions to Algebra and Geometry, 35 (1994), pp. 125–129
53. J. PACH AND P. K. AGARWAL, *Combinatorial Geometry*, J. Wiley and Sons, New York, 1995
54. A. PAFFENHOLZ, *The E-construction applied to products*, Webpage with polymake data files, TU Berlin 2004, <http://www.math.tu-berlin.de/~paffenho/2s2spages.shtml>
55. ———, *New polytopes from products*, Preprint, TU Berlin, 22 pages, November 2004, arXiv:math.MG/0411092
56. A. PAFFENHOLZ AND A. WERNER, *Constructions for 4-polytopes and the cone of flag vectors*, Preprint, TU Berlin, November 2005, 20 pages, <http://arXiv.org/math/0511751>
57. A. PAFFENHOLZ AND G. M. ZIEGLER, *The  $E_t$ -construction for lattices, spheres and polytopes*, Discrete & Computational Geometry (Billera Festschrift: M. Bayer, C. Lee, B. Sturmfels, eds.), 32 (2004), pp. 601–624, <http://www.arXiv.org/math.MG/0304492>
58. K. POLTHIER, S. KHADEM-AL-CHARIEH, E. PREUSS, AND U. REITEBUCH, *JavaView visualization software, 1999-2004*, <http://www.javaview.de>
59. A. RIBÓ MOR, *Realization and Counting Problems for Planar Structures: Trees and Linkages, Polytopes and Polyominoes*, PhD thesis, FU Berlin, 2005, 23+167 pages
60. J. RICHTER-GEBERT, *Realization Spaces of Polytopes*, vol. 1643 of Lecture Notes in Mathematics, Springer-Verlag, Berlin Heidelberg, 1996
61. G. ROTE, *The number of spanning trees in a planar graph*, Oberwolfach Reports, 2 (2005), pp. 969–973
62. R. SANYAL, *On the combinatorics of projected deformed products*, Diplomarbeit, TU Berlin, 2005, 57 pages
63. R. SANYAL, T. SCHRÖDER, AND G. M. ZIEGLER, *Polytopes and polyhedral surfaces via projection*, Preprint in preparation, TU Berlin 2005
64. G. SCHAEFFER, *Random sampling of large planar maps and convex polyhedra*, in Annual ACM Symposium on Theory of Computing (Atlanta, GA, 1999), ACM, New York, 1999, pp. 760–769
65. D. SCHATTSCHNEIDER AND M. SENECHAL, *Tilings*, in Handbook of Discrete and Computational Geometry, J. E. Goodman and J. O'Rourke, eds., Chapman & Hall/CRC Press, Boca Raton, second ed., 2004, ch. 3, pp. 53–72
66. L. SCHLÄFLI, *Theorie der vielfachen Kontinuität*, Denkschriften der Schweizerischen naturforschenden Gesellschaft, Vol. 38, pp. 1–237, Zürcher und Furrer, Zürich, 1901. Written 1850-1852. Reprinted in: Ludwig Schläfli, 1814-1895, Gesammelte Mathematische Abhandlungen Vol. I, Birkhäuser, Basel 1950, pp. 167–387
67. V. SCHLEGEL, *Theorie der homogen zusammengesetzten Raumgebilde*, Nova Acta Leop. Carol. (Verhandlungen der Kaiserlichen Leopoldinisch-Carolinischen Deutschen Akademie der Naturforscher, Halle), 44 (1883), pp. 343–459, W. Engelmann, Leipzig



68. B. A. SPRINGBORN, *A unique representation theorem of polyhedral types: Centering via Möbius transformations*, Math. Zeitschrift, 249 (2005), pp. 513–517, <http://www.arXiv.org/math.MG/0401005>
69. R. P. STANLEY, *The number of faces of simplicial polytopes and spheres*, in Discrete Geometry and Convexity (New York 1982), J. E. Goodman, E. Lutwak, J. Malkevitch, and R. Pollack, eds., vol. 440 of Annals of the New York Academy of Sciences, 1985, pp. 212–223
70. ———, *Generalized h-vectors, intersection cohomology of toric varieties, and related results*, in Commutative Algebra and Combinatorics, M. Nagata and H. Matsumura, eds., vol. 11 of Advanced Studies in Pure Mathematics, Kinokuniya, Tokyo, 1987, pp. 187–213
71. R. P. STANLEY, *Log-concave and unimodal sequences in algebra, combinatorics, and geometry*, in Graph theory and its applications: East and West (Jinan, 1986), vol. 576 of Ann. New York Acad. Sci., New York Acad. Sci., New York, 1989, pp. 500–535
72. G. STEIN, *Realisierung von 3-Polytopen*, Diplomarbeit, TU Berlin, 2000, in German, 100 pages
73. E. STEINITZ, *Über die Eulerschen Polyederrelationen*, Archiv für Mathematik und Physik, 11 (1906), pp. 86–88
74. ———, *Polyeder und Raumeinteilungen*, in Encyklopädie der mathematischen Wissenschaften, Geometrie, III.1.2., Heft 9, Kapitel III A B 12, W. F. Meyer and H. Mohrmann, eds., B. G. Teubner, Leipzig, 1922, pp. 1–139
75. E. STEINITZ AND H. RADEMACHER, *Vorlesungen über die Theorie der Polyeder*, Springer-Verlag, Berlin, 1934. Reprint, Springer-Verlag 1976
76. W. P. THURSTON, *Geometry and Topology of 3-Manifolds*, Lecture Notes, Princeton University, Princeton 1977–1978
77. W. T. TUTTE, *How to draw a graph*, Proc. London Math. Soc. (3), 13 (1963), pp. 743–767
78. A. WERNER, *Unimodality and convexity of f-vectors of polytopes*, Preprint, TU Berlin, December 2005, <http://www.arXiv.org/math.CO/0512131>
79. G. M. ZIEGLER, *Lectures on Polytopes*, vol. 152 of Graduate Texts in Mathematics, Springer-Verlag, New York, 1995. Revised edition, 1998; “Updates, corrections, and more” at <http://www.math.tu-berlin.de/~ziegler>
80. ———, *Face numbers of 4-polytopes and 3-spheres*, in Proceedings of the International Congress of Mathematicians (ICM 2002, Beijing), L. Tatsien, ed., vol. III, Beijing, China, 2002, Higher Education Press, pp. 625–634, <http://www.arXiv.org/math.MG/0208073>
81. ———, *Projected products of polygons*, Electronic Research Announcements AMS, 10 (2004), pp. 122–134, <http://www.arXiv.org/math.MG/0407042>